


Review

Recent Advances in Grayanane Diterpenes: Isolation, Structural Diversity, and Bioactivities from Ericaceae Family (2018–2024)

Sheng Liu ^{1,†}, Lili Sun ^{2,†}, Peng Zhang ² and Changshan Niu ^{2,*} ¹ School of Pharmacy, Yantai University, Yantai 264005, China; liusheng87@126.com² College of Pharmacy, University of Utah, Salt Lake City, UT 84108, USA; lili.sun1989@gmail.com (L.S.); u6024660@utah.edu (P.Z.)

* Correspondence: niucs88@gmail.com

† These authors contributed equally to this work.

Abstract: Diterpenes represent one of the most diverse and structurally complex families of natural products. Among the myriad of diterpenoids, grayanane diterpenes are particularly notable. These terpenes are characterized by their unique 5/7/6/5 tetracyclic system and are exclusive to the Ericaceae family of plants. Renowned for their complex structures and broad spectrum of bioactivities, grayanane diterpenes have become a primary focus in extensive phytochemical and pharmacological research. Recent studies, spanning from 2018 to January 2024, have reported a series of new grayanane diterpenes with unprecedented carbon skeletons. These compounds exhibit various biological properties, including analgesic, antifeedant, anti-inflammatory, and inhibition of protein tyrosine phosphatase 1B (PTP1B). This paper delves into the discovery of 193 newly identified grayanoids, representing 15 distinct carbon skeletons within the Ericaceae family. The study of grayanane diterpenes is not only a deep dive into the complexities of natural product chemistry but also an investigation into potential therapeutic applications. Their unique structures and diverse biological actions make them promising candidates for drug discovery and medicinal applications. The review encompasses their occurrence, distribution, structural features, and biological activities, providing invaluable insights for future pharmacological explorations and research.



Citation: Liu, S.; Sun, L.; Zhang, P.; Niu, C. Recent Advances in Grayanane Diterpenes: Isolation, Structural Diversity, and Bioactivities from Ericaceae Family (2018–2024). *Molecules* **2024**, *29*, 1649. <https://doi.org/10.3390/molecules29071649>

Academic Editors: Md Saifullah, Quan V. Vuong and Mohammad Rezaul Islam Shishir

Received: 28 February 2024

Revised: 20 March 2024

Accepted: 4 April 2024

Published: 6 April 2024



Copyright: © 2024 by the authors. Licensee MDPI, Basel, Switzerland. This article is an open access article distributed under the terms and conditions of the Creative Commons Attribution (CC BY) license (<https://creativecommons.org/licenses/by/4.0/>).

Keywords: diterpene; grayanane; Ericaceae family; *Pieris*; *Rhododendron*; *Kalmia*; *Craibiodendron*; *Leucothoe*; pain assay; PTP1B; anti-inflammatory; analgesic; antifeedant

1. Introduction

Diterpenes, a class of terpenoids consisting of four isoprene units, represent one of the most diverse and structurally complex families of natural products. As a prominent family of natural products, diterpenes are predominantly found in plants, where they play vital roles in various biological processes, from defense mechanisms against herbivores and pathogens to growth regulation [1]. The vast structural diversity and the array of bioactivities associated with diterpenes have made diterpenes a focal point of intense scientific research.

Among the myriad of diterpenes, grayanane diterpenes stand out as particularly noteworthy. These terpenes are distinguished by their unique and intricate 5/7/6/5 tetracyclic system and are exclusive to the Ericaceae family of plants [2–4]. The Ericaceae family, which encompasses about 4000 species spread across 126 genera, ranging from small herbs to large trees, is a rich source of terpenoids, including triterpenoids, meroterpenoids, and especially diterpenoids such as grayanane diterpenes [2,5]. Grayanane diterpenes, as characteristic secondary metabolites of the Ericaceae family, are prominently found in genera like *Pieris*, *Rhododendron*, *Kalmia*, *Craibiodendron*, and *Leucothoe*.

The structural complexity and diversity of grayanane diterpenes are notable, with over 400 compounds encompassing 25 carbon skeletons that have been isolated and identified

from the Ericaceae family [2,6,7]. These compounds are recognized for their wide-ranging bioactivities, including analgesic [3,8], anti-inflammatory [9], antifedant [10], and protein tyrosine phosphatase 1B (PTP1B) [11] inhibitory activities. Their unique chemical structures and significant biological activities have increasingly attracted the interest of organic synthesis chemists [12,13].

Despite several reviews that have covered aspects of grayanane diterpenoids, a comprehensive and in-depth overview of the developments and discoveries in this field, especially from 2018 to January 2024, has been lacking [2,6,7,14–16]. This review aims to fill that gap by focusing on the recent advancements made in the isolation, structural elucidation, and bioactivity studies of these diterpenes. Through a detailed examination of various species within the Ericaceae family, the paper presents a thorough overview of their occurrence, distribution, structural features, and biological activities. This approach offers valuable insights for ongoing pharmacological research and underscores the growing significance of grayanane diterpenes in the field of natural product chemistry.

2. Overview of Structural Diversity and Biological Activities of Grayanane Terpenes

After an exhaustive search of the PubMed, SciFinder, Scopus, and Google Scholar databases, utilizing the keywords “grayanane”, “diterpenes”, “diterpenoids”, and “Ericaceae family” from 2018 to January 2024, a remarkable total of 193 novel grayanane diterpenes were isolated and identified from the Ericaceae family plants. These discoveries predominantly came from the roots, leaves, or flowers of *Pieris*, *Rhododendron*, and *Craibiodendron* genus. These novel grayanane diterpenes are categorized into 15 distinct carbon skeletons, including *ent*-kaurane [17], 4,5-*seco*-kaurane [18], *A-home-B-nor-ent*-kaurane [17], grayanane [10], 1,5-*seco*-grayanane [19,20], 1,10-*seco*-grayanane [17], 1,10:2,3-*diseco*-grayanane [17,21], mollane [20,21], kalmene [19,20,22], 1,5-*seco*-kalmene [23], leucothane [18,21,23–25], rhomollane [23], micranthane [20,25], mollebenzylane [26], and rhodauricane [19], as illustrated in Figure 1.

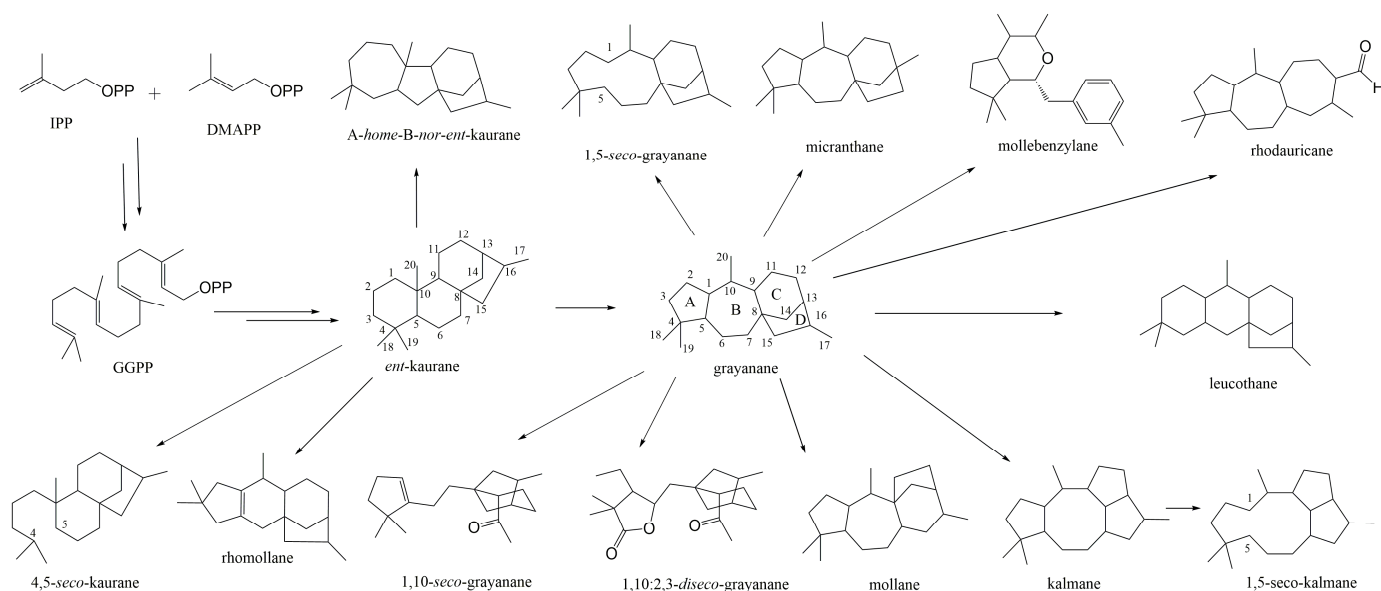


Figure 1. Representation of grayanane-related carbon skeletons. The core 5/7/6/5 skeleton of grayanane was labeled as rings A, B, C, and D.

Most of the literature research has focused on the bioactive potential of these compounds. A significant part of the studies is dedicated to analyzing their analgesic effects *in vivo*, particularly in mouse models. Various models have been employed for this purpose, including the acetic acid-induced writhing test and the capsaicin- and AITC-induced writhing test model [27]. Additionally, there have been studies on the antifedant activity using *Plutella xylostella* [10], ion channel testing on Nav1.7 and KCNQ2 [10], anti-inflammatory

properties [11], cytotoxicity [11], and PTP1B activity [11]. In the subsequent sections of the study, an in-depth exploration of the phytochemistry of these compounds is conducted. For detailed compound information, including the compounds' original name, their occurrence, distribution, and publication references, please see Table 1. The bioactivities reported in the references were summarized in Table 2.

Table 1. Compound Names, Plant Sources, Related References, and Year of Publication.

No.	Name	Plant Resource	Year	Ref.
1	Pierisformosoid A	<i>Pieris formosa</i> , roots	2018	[8]
2	Pierisformosoid B	<i>Pieris formosa</i> , roots	2018	[8]
3	Pierisformosoid C	<i>Pieris formosa</i> , roots	2018	[8]
4	Pierisformosoid D	<i>Pieris formosa</i> , roots	2018	[8]
5	Pierisformosoid E	<i>Pieris formosa</i> , roots	2018	[8]
6	Pierisformosoid F	<i>Pieris formosa</i> , roots	2018	[8]
7	Pierisformosoid G	<i>Pieris formosa</i> , roots	2018	[8]
8	Pierisformosoid H	<i>Pieris formosa</i> , roots	2018	[8]
9	Pierisformosoid I	<i>Pieris formosa</i> , roots	2018	[8]
10	Pierisformosoid J	<i>Pieris formosa</i> , roots	2018	[8]
11	Pierisformosoid K	<i>Pieris formosa</i> , roots	2018	[8]
12	Pierisformosoid L	<i>Pieris formosa</i> , roots	2018	[8]
13	3-epi-grayanoside B	<i>Rhododendron micranthum</i> , leaves	2018	[9]
14	Micranthanoside A	<i>Rhododendron micranthum</i> , leaves	2018	[9]
15	Micranthanoside B	<i>Rhododendron micranthum</i> , leaves	2018	[9]
16	Micranthanoside C	<i>Rhododendron micranthum</i> , leaves	2018	[9]
17	Micranthanoside D	<i>Rhododendron micranthum</i> , leaves	2018	[9]
18	Micranthanoside E	<i>Rhododendron micranthum</i> , leaves	2018	[9]
19	hydroxygrayanoside C	<i>Rhododendron micranthum</i> , leaves	2018	[9]
20	micranthanoside F	<i>Rhododendron micranthum</i> , leaves	2018	[9]
21	14 β -acetyoxymicranthanoside	<i>Rhododendron micranthum</i> , leaves	2018	[9]
22	micranthanoside G	<i>Rhododendron micranthum</i> , leaves	2018	[9]
23	14-Oacetylmicranthanoside G	<i>Rhododendron micranthum</i> , leaves	2018	[9]
24	14 β -hydroxypieroside A	<i>Rhododendron micranthum</i> , leaves	2018	[9]
25	micranthanoside H	<i>Rhododendron micranthum</i> , leaves	2018	[9]
26	Mollfoliagin D	<i>Rhododendron molle</i> , leaves	2018	[7]
27	6-O-Acetyl rhodomollein XI	<i>Rhododendron molle</i> , leaves	2018	[7]
28	Mollfoliagin F	<i>Rhododendron molle</i> , leaves	2018	[7]
29	18-Hydroxygrayanotoxin XVIII	<i>Rhododendron molle</i> , leaves	2018	[7]
30	2-O-Methyl rhodomollein I	<i>Rhododendron molle</i> , leaves	2018	[7]
31	2-O-Methyl rhodomollein XII	<i>Rhododendron molle</i> , leaves	2018	[7]
32	2-O-Methyl rhodojaponin VI	<i>Rhododendron molle</i> , leaves	2018	[7]
33	2-O-Methyl rhodojaponin VII	<i>Rhododendron molle</i> , leaves	2018	[7]
34	Rhododecorumin VIII	<i>Rhododendron decorum</i> , leaves and twigs	2018	[22]
35	Rhododecorumin IX	<i>Rhododendron decorum</i> , leaves and twigs	2018	[22]
36	Rhododecorumin X	<i>Rhododendron decorum</i> , leaves and twigs	2018	[22]
37	Rhododecorumin XI	<i>Rhododendron decorum</i> , leaves and twigs	2018	[22]
38	Rhododecorumin XII	<i>Rhododendron decorum</i> , leaves and twigs	2018	[22]
39	Rhododeoside I	<i>Rhododendron decorum</i> , leaves and twigs	2018	[22]
40	Rhodoauriculatol I	<i>Rhododendron auriculatum</i> , leaves	2019	[21]
41	Rhodomicrosideside F	<i>Rhododendron auriculatum</i> , leaves	2019	[14]
42	Rhodomicrosideside G	<i>Rhododendron auriculatum</i> , leaves	2019	[14]
43	Rhodomicrosideside H	<i>Rhododendron auriculatum</i> , leaves	2019	[14]
44	Rhodomicrosideside I	<i>Rhododendron auriculatum</i> , leaves	2019	[14]
45	Auriculatol B	<i>Rhododendron auriculatum</i> , leaves	2019	[25]
46	3-epi-Grayanotoxin XVIII	<i>Rhododendron auriculatum</i> , leaves	2019	[25]
47	6-Deoxycraibiotoxin I	<i>Rhododendron auriculatum</i> , leaves	2019	[25]
48	3-epi-Auriculatol B	<i>Rhododendron auriculatum</i> , leaves	2019	[25]
49	19-Hydroxy-3-epi-auriculatol B	<i>Rhododendron auriculatum</i> , leaves	2019	[25]
50	Auriculatol C	<i>Rhododendron auriculatum</i> , leaves	2019	[25]
51	Auriculatol D	<i>Rhododendron auriculatum</i> , leaves	2019	[25]
52	Auriculatol E	<i>Rhododendron auriculatum</i> , leaves	2019	[25]
53	Auriculatol F	<i>Rhododendron auriculatum</i> , leaves	2019	[25]
54	2 α -Hydroxyauriculatol F	<i>Rhododendron auriculatum</i> , leaves	2019	[25]
55	1-epi-Pieristoxin S	<i>Rhododendron auriculatum</i> , leaves	2019	[25]
56	17-Hydroxygrayanotoxin XIX	<i>Pieris japonica</i> , leaves	2019	[26]
57	2-O-Methyl rhodomollein XIX	<i>Pieris japonica</i> , leaves	2019	[26]
58	17-Hydroxy-3-epi-auriculatol B	<i>Pieris japonica</i> , leaves	2019	[26]
59	Pierisjaponol A	<i>Pieris japonica</i> , leaves	2019	[26]
60	Pierisjaponol B	<i>Pieris japonica</i> , leaves	2019	[26]

Table 1. Cont.

No.	Name	Plant Resource	Year	Ref.
61	13 α -Hydroxyrhodomollein XVII	<i>Pieris japonica</i> , leaves	2019	[26]
62	12 β -Hydroxygrayanotoxin XVIII	<i>Pieris japonica</i> , leaves	2019	[26]
63	2 α -Hydroxyasebotoxin II	<i>Pieris japonica</i> , leaves	2019	[26]
64	2 α -O-Methylgrayanotoxin II	<i>Pieris japonica</i> , leaves	2019	[26]
65	Pierisjaponol C	<i>Pieris japonica</i> , leaves	2019	[26]
66	16-O-Methylgrayanotoxin XVIII	<i>Pieris japonica</i> , leaves	2019	[26]
67	Pierisjaponol D	<i>Pieris japonica</i> , leaves	2019	[26]
68	Rhodomollein XLIV	<i>Rhododendron molle</i> , flowers	2020	[20]
69	Rhodomollein XLV	<i>Rhododendron molle</i> , flowers	2020	[20]
70	Rhodomollein XLVI	<i>Rhododendron molle</i> , flowers	2020	[20]
71	Rhodomollein XLVII	<i>Rhododendron molle</i> , flowers	2020	[20]
72	Rhodomollein XLIX	<i>Rhododendron molle</i> , flowers	2020	[20]
73	Rhodomollein L	<i>Rhododendron molle</i> , flowers	2020	[20]
74	Dauricanol A	<i>Rhododendron dauricum</i> , flowers	2023	[16]
75	Dauricanol B	<i>Rhododendron dauricum</i> , flowers	2023	[16]
76	Dauricanol C	<i>Rhododendron dauricum</i> , flowers	2023	[16]
77	Daublossomin G	<i>Rhododendron dauricum</i> , flowers	2023	[27]
78	Daublossomin H	<i>Rhododendron dauricum</i> , flowers	2023	[27]
79	Daublossomin I	<i>Rhododendron dauricum</i> , flowers	2023	[27]
80	Daublossomin J	<i>Rhododendron dauricum</i> , flowers	2023	[27]
81	Daublossomin K	<i>Rhododendron dauricum</i> , flowers	2023	[27]
82	Daublossomin L	<i>Rhododendron dauricum</i> , flowers	2023	[27]
83	Daublossomin M	<i>Rhododendron dauricum</i> , flowers	2023	[27]
84	Craibiodenoside A	<i>Craibiodendron yunnanense</i> , leaves	2023	[28]
85	Craibiodenoside B	<i>Craibiodendron yunnanense</i> , leaves	2023	[28]
86	Craibiodenoside C	<i>Craibiodendron yunnanense</i> , leaves	2023	[28]
87	Molleblossomin G	<i>Rhododendron molle</i> , flowers	2024	[29]
88	Molleblossomin H	<i>Rhododendron molle</i> , flowers	2024	[29]
89	Molleblossomin I	<i>Rhododendron molle</i> , flowers	2024	[29]
90	Molleblossomin J	<i>Rhododendron molle</i> , flowers	2024	[29]
91	Molleblossomin K	<i>Rhododendron molle</i> , flowers	2024	[29]
92	Molleblossomin L	<i>Rhododendron molle</i> , flowers	2024	[29]
93	16-Acetylgrayanotoxin III	<i>Rhododendron micranthum</i> , roots	2020	[19]
94	3 β , 6 β , 16 α -trihydroxy-14b-acetoxy-grayan-1(5), 10(20)-diene	<i>Rhododendron micranthum</i> , roots	2020	[19]
95	14 β -(2-Hydroxypropanoyloxy)rhodomollein XVII	<i>Craibiodendron yunnanense</i> , leaves	2023	[30]
96	2-O-Ethoxyrhodojaponin VI	<i>Craibiodendron yunnanense</i> , leaves	2023	[30]
97	Micranthanoside J	<i>Craibiodendron yunnanense</i> , leaves	2023	[30]
98	Mollfoliagein A	<i>Rhododendron molle</i> , leaves	2018	[7]
99	Mollfoliagein B	<i>Rhododendron molle</i> , leaves	2018	[7]
100	Mollfoliagein C	<i>Rhododendron molle</i> , leaves	2018	[7]
101	6-O-Acetyl rhodomollein XXXI	<i>Rhododendron molle</i> , leaves	2018	[7]
102	Mollfoliagein E	<i>Rhododendron molle</i> , leaves	2018	[7]
103	Rhododecorumin VI	<i>Rhododendron decorum</i> , leaves and twigs	2018	[22]
104	Rhododecorumin VII	<i>Rhododendron decorum</i> , leaves and twigs	2018	[22]
105	Epoxyperistoxin A	<i>Pieris formosa</i> , roots	2019	[31]
106	Epoxyperistoxin B	<i>Pieris formosa</i> , roots	2019	[31]
107	Epoxyperistoxin C	<i>Pieris formosa</i> , roots	2019	[31]
108	Epoxyperistoxin D	<i>Pieris formosa</i> , roots	2019	[31]
109	Epoxyperistoxin E	<i>Pieris formosa</i> , roots	2019	[31]
110	Epoxyperistoxin F	<i>Pieris formosa</i> , roots	2019	[31]
111	Epoxyperistoxin G	<i>Pieris formosa</i> , roots	2019	[31]
112	Epoxyperistoxin H	<i>Pieris formosa</i> , roots	2019	[31]
113	14-Deoxyrhodomollein XXXVII	<i>Pieris japonica</i> , leaves	2019	[26]
114	Rhodomollein XLVIII	<i>Rhododendron molle</i> , flowers	2020	[20]
115	Micranthanol A	<i>Rhododendron micranthum</i> , leaves	2021	[17]
116	Micranthanol B	<i>Rhododendron micranthum</i> , leaves	2021	[17]
117	Daublossomin A	<i>Rhododendron dauricum</i> , flowers	2023	[27]
118	Daublossomin B	<i>Rhododendron dauricum</i> , flowers	2023	[27]
119	Daublossomin C	<i>Rhododendron dauricum</i> , flowers	2023	[27]
120	Daublossomin D	<i>Rhododendron dauricum</i> , flowers	2023	[27]
121	Daublossomin E	<i>Rhododendron dauricum</i> , flowers	2023	[27]
122	Daublossomin F	<i>Rhododendron dauricum</i> , flowers	2023	[27]
123	Craibiodenoside D	<i>Craibiodendron yunnanense</i> , leaves	2023	[28]
124	Craibiodenoside E	<i>Craibiodendron yunnanense</i> , leaves	2023	[28]
125	Craibiodenoside F	<i>Craibiodendron yunnanense</i> , leaves	2023	[28]
126	Molleblossomin A	<i>Rhododendron molle</i> , flowers	2024	[29]

Table 1. Cont.

No.	Name	Plant Resource	Year	Ref.
127	Molleblossomin B	<i>Rhododendron molle</i> , flowers	2024	[29]
128	Molleblossomin C	<i>Rhododendron molle</i> , flowers	2024	[29]
129	Molleblossomin D	<i>Rhododendron molle</i> , flowers	2024	[29]
130	Molleblossomin E	<i>Rhododendron molle</i> , flowers	2024	[29]
131	Molleblossomin F	<i>Rhododendron molle</i> , flowers	2024	[29]
132	Auriculatol A	<i>Rhododendron auriculatum</i> , leaves	2019	[25]
133	9 β -Hydroxy-1,5-seco-grayanotoxin	<i>Rhododendron micranthum</i> , leaves	2021	[17]
134	Dauricanol D	<i>Rhododendron dauricum</i> , flowers	2023	[16]
135	Dauricanol E	<i>Rhododendron dauricum</i> , flowers	2023	[16]
136	Pierisjaponin A	<i>Pieris japonica</i> , leaves	2020	[18]
137	Pierisjaponin B	<i>Pieris japonica</i> , leaves	2020	[18]
138	Rhodoauriculatol A	<i>Rhododendron auriculatum</i> , leaves	2019	[21]
139	Rhodoauriculatol B	<i>Rhododendron auriculatum</i> , leaves	2019	[21]
140	Rhodoauriculatol C	<i>Rhododendron auriculatum</i> , leaves	2019	[21]
141	Rhodoauriculatol D	<i>Rhododendron auriculatum</i> , leaves	2019	[21]
142	Pierisjaponin J	<i>Pieris japonica</i> , leaves	2020	[18]
143	Birhodomollein D	<i>Rhododendron pumilum</i> , fruits	2018	[32]
144	Birhodomollein E	<i>Rhododendron pumilum</i> , fruits	2018	[32]
145	Bimollfoliagein A	<i>Rhododendron molle</i> , leaves	2018	[7]
146	Rhodomollein XLIII	<i>Rhododendron molle</i> , flowers	2020	[20]
147	Bismollether A	<i>Rhododendron molle</i> , flowers	2022	[24]
148	Bismollether B	<i>Rhododendron molle</i> , flowers	2022	[24]
149	Bismollether C	<i>Rhododendron molle</i> , flowers	2022	[24]
150	Rhododecorumin I	<i>Rhododendron decorum</i> , leaves and twigs	2018	[22]
151	Rhododecorumin II	<i>Rhododendron decorum</i> , leaves and twigs	2018	[22]
152	Rhododecorumin III	<i>Rhododendron decorum</i> , leaves and twigs	2018	[22]
153	Rhodoauriculatol G	<i>Rhododendron auriculatum</i> , leaves	2019	[21]
154	Rhodoauriculatol H	<i>Rhododendron auriculatum</i> , leaves	2019	[21]
155	Rhodomicranoside A	<i>Rhododendron auriculatum</i> , leaves	2019	[14]
156	Rhodomicranoside B	<i>Rhododendron auriculatum</i> , leaves	2019	[14]
157	Rhodomicranoside C	<i>Rhododendron auriculatum</i> , leaves	2019	[14]
158	Rhodomollein LII	<i>Rhododendron molle</i> , flowers	2020	[20]
159	Rhodomollein LIII	<i>Rhododendron molle</i> , flowers	2020	[20]
160	3 β ,7 α ,14 β -trihydroxy-leucoth-10(20),15-dien-5-one	<i>Pieris formosa</i> , roots	2020	[15]
161	10 α ,16 α -dihydroxy-leucoth-5-one	<i>Pieris formosa</i> , roots	2020	[15]
162	Pierisjaponin F	<i>Pieris japonica</i> , leaves	2020	[18]
163	Pierisjaponin G	<i>Pieris japonica</i> , leaves	2020	[28]
164	Rhodoauriculatol F	<i>Rhododendron auriculatum</i> , leaves	2019	[21]
165	Pierisentkauran B	<i>Pieris formosa</i> , roots	2020	[15]
166	Pierisentkauran C	<i>Pieris formosa</i> , roots	2020	[15]
167	Pierisentkauran D	<i>Pieris formosa</i> , roots	2020	[15]
168	Pierisentkauran E	<i>Pieris formosa</i> , roots	2020	[15]
169	Rhodomicranoside D	<i>Rhododendron micranthum</i> , leaves	2019	[14]
170	Rhodomicranoside E	<i>Rhododendron micranthum</i> , leaves	2019	[14]
171	Pierisentkauran F	<i>Pieris formosa</i> , roots	2020	[15]
172	Pierisjaponin H	<i>Pieris japonica</i> , leaves	2020	[18]
173	Pierisjaponin I	<i>Pieris japonica</i> , leaves	2020	[18]
174	8 α -O-Acetyl-rhodomollein XXIII	<i>Rhododendron micranthum</i> , leaves	2021	[17]
175	Rhodokalmanol A	<i>Rhododendron dauricum</i> , leaves	2022	[33]
176	Rhodokalmanol B	<i>Rhododendron dauricum</i> , leaves	2022	[33]
177	Rhodokalmanol C	<i>Rhododendron dauricum</i> , leaves	2022	[33]
178	Rhodokalmanol D	<i>Rhododendron dauricum</i> , leaves	2022	[33]
179	16 α -acetoxy rhodomollein XXIII	<i>Rhododendron micranthum</i> , roots	2020	[19]
180	Rhodomollein LI	<i>Rhododendron molle</i> , flowers	2020	[20]
181	Rhodoauriculatol E	<i>Rhododendron auriculatum</i> , leaves	2019	[21]
182	Mollebenzylanol A	<i>Rhododendron molle</i> , leaves	2018	[23]
183	Mollebenzylanol B	<i>Rhododendron molle</i> , leaves	2018	[23]
184	Rhododecorumin IV	<i>Rhododendron decorum</i> , leaves and twigs	2018	[22]
185	Rhododecorumin V	<i>Rhododendron decorum</i> , leaves and twigs	2018	[22]
186	Micranthanone B	<i>Rhododendron micranthum</i> , leaves	2021	[17]
187	Micranthanone C	<i>Rhododendron micranthum</i> , leaves	2021	[17]
188	14-epi-Mollanol A	<i>Rhododendron micranthum</i> , leaves	2021	[17]
189	Mollanol B	<i>Rhododendron micranthum</i> , leaves	2021	[17]
190	Mollanol C	<i>Rhododendron micranthum</i> , leaves	2021	[17]
191	Pierisjaponin E	<i>Pieris japonica</i> , leaves	2020	[18]
192	Rhomollone A	<i>Rhododendron molle</i> , flowers	2020	[20]
193	rhodauricanol A	<i>Rhododendron dauricum</i> , flowers	2023	[16]

Table 2. Compound Names and Their Reported Activities.

No	In Vivo		In Vitro	
	Test Mode	Activity/Dose	Test Model	Activity/Dose
1	Acetic acid-induced pain mouse model <i>Plutella xylostella</i>	Analgesic, 5 mg/kg Antifeedant, 0.5 mg/mL	Nav1.7 channel KCNQ2 channel	ND, 10 μ M ND, 10 μ M
2	Acetic acid-induced pain mouse model	Analgesic, 1 mg/kg	Nav1.7 channel KCNQ2 channel	ND, 10 μ M ND, 10 μ M
3	-	-	Nav1.7 channel KCNQ2 channel	ND, 10 μ M ND, 10 μ M
4	Acetic acid-induced pain mouse model <i>Plutella xylostella</i>	Analgesic, 0.1 mg/kg Antifeedant, 0.5 mg/mL	Nav1.7 channel KCNQ2 channel	ND, 10 μ M 38.3% inhibitory, 10 μ M
5	Acetic acid-induced pain mouse model	Analgesic, 5 mg/kg	Nav1.7 channel KCNQ2 channel	ND, 10 μ M ND, 10 μ M
6	-	-	Nav1.7 channel KCNQ2 channel	ND, 10 μ M ND, 10 μ M
7	Acetic acid-induced pain mouse model	Analgesic, 0.1 mg/kg	Nav1.7 channel KCNQ2 channel	ND, 10 μ M ND, 10 μ M
8	Acetic acid-induced pain mouse model	Analgesic, 5 mg/kg	Nav1.7 channel KCNQ2 channel	ND, 10 μ M ND, 10 μ M
9	Acetic acid-induced pain mouse model <i>Plutella xylostella</i>	ND Antifeedant, 0.5 mg/mL	Nav1.7 channel KCNQ2 channel	ND, 10 μ M ND, 10 μ M
10	Acetic acid-induced pain mouse model	ND	Nav1.7 channel KCNQ2 channel	ND, 10 μ M ND, 10 μ M
11	Acetic acid-induced pain mouse model	ND	Nav1.7 channel KCNQ2 channel	ND, 10 μ M ND, 10 μ M
12	Acetic acid-induced pain mouse model	ND	Nav1.7 channel KCNQ2 channel	ND, 10 μ M ND, 10 μ M
13	Acetic acid-induced pain mouse model	Analgesic, 5.0 mg/kg	Anti-inflammatory Cytotoxicity PTP1B	ND, 40 μ M ND, 40 μ M ND, 40 μ M
14	Acetic acid-induced pain mouse model	Analgesic, 0.2 mg/kg	Anti-inflammatory Cytotoxicity PTP1B	ND, 40 μ M ND, 40 μ M ND, 40 μ M
15	Acetic acid-induced pain mouse model	Analgesic, 1.0 mg/kg	Anti-inflammatory Cytotoxicity PTP1B	ND, 40 μ M ND, 40 μ M ND, 40 μ M
16	Acetic acid-induced pain mouse model	Analgesic, 5.0 mg/kg	Anti-inflammatory Cytotoxicity PTP1B	ND, 40 μ M ND, 40 μ M ND, 40 μ M
17	Acetic acid-induced pain mouse model	Analgesic, 5.0 mg/kg	Anti-inflammatory Cytotoxicity PTP1B	ND, 40 μ M ND, 40 μ M ND, 40 μ M
18	Acetic acid-induced pain mouse model	Analgesic, 5.0 mg/kg	Anti-inflammatory Cytotoxicity PTP1B	ND, 40 μ M ND, 40 μ M ND, 40 μ M
19	Acetic acid-induced pain mouse model	Analgesic, 1.0 mg/kg	Anti-inflammatory Cytotoxicity PTP1B	ND, 40 μ M ND, 40 μ M ND, 40 μ M
20	Acetic acid-induced pain mouse model	Analgesic, 5.0 mg/kg	Anti-inflammatory Cytotoxicity PTP1B	ND, 40 μ M ND, 40 μ M ND, 40 μ M
21	Acetic acid-induced pain mouse model	Analgesic, 5.0 mg/kg	Anti-inflammatory Cytotoxicity PTP1B	ND, 40 μ M ND, 40 μ M ND, 40 μ M
22	Acetic acid-induced pain mouse model	Analgesic, 5.0 mg/kg	Anti-inflammatory Cytotoxicity PTP1B	ND, 40 μ M ND, 40 μ M ND, 40 μ M

Table 2. Cont.

No	In Vivo		In Vitro	
	Test Mode	Activity/Dose	Test Model	Activity/Dose
23	Acetic acid-induced pain mouse model	Analgesic, 5.0 mg/kg	Anti-inflammatory Cytotoxicity PTP1B	ND, 40 μ M ND, 40 μ M ND, 40 μ M
24	Acetic acid-induced pain mouse model	Analgesic, 5.0 mg/kg	Anti-inflammatory Cytotoxicity PTP1B	ND, 40 μ M ND, 40 μ M ND, 40 μ M
25	Acetic acid-induced pain mouse model	Analgesic, 5.0 mg/kg	Anti-inflammatory Cytotoxicity PTP1B	ND, 40 μ M ND, 40 μ M ND, 40 μ M
26	-	-	Anti-inflammatory	ND, 40 μ M
27	-	-	Anti-inflammatory	ND, 40 μ M
28	-	-	Anti-inflammatory	ND, 40 μ M
29	-	-	Anti-inflammatory	ND, 40 μ M
30	-	-	Anti-inflammatory	ND, 40 μ M
31	-	-	Anti-inflammatory	ND, 40 μ M
32	-	-	Anti-inflammatory	ND, 40 μ M
33	-	-	Anti-inflammatory	ND, 40 μ M
34	Acetic acid-induced pain mouse model	Analgesic, 10.0 mg/kg	-	-
35	-	-	-	-
36	Acetic acid-induced pain mouse model	Analgesic, 10.0 mg/kg	-	-
37	Acetic acid-induced pain mouse model	Analgesic, 10.0 mg/kg	-	-
38	Acetic acid-induced pain mouse model	Analgesic, 0.8 mg/kg	-	-
39	Acetic acid-induced pain mouse model	Analgesic, 10.0 mg/kg	-	-
40	Acetic acid-induced pain mouse model	Analgesic, 1.0 mg/kg	-	-
41	Acetic acid-induced pain mouse model	Analgesic, 5.0 mg/kg	-	-
42	Acetic acid-induced pain mouse model	Analgesic, 5.0 mg/kg	-	-
43	Acetic acid-induced pain mouse model	Analgesic, 1.0 mg/kg	-	-
44	Acetic acid-induced pain mouse model	Analgesic, 1.0 mg/kg	-	-
45	Acetic acid-induced pain mouse model	Analgesic, 5.0 mg/kg	-	-
46	Acetic acid-induced pain mouse model	Analgesic, 5.0 mg/kg	-	-
47	Acetic acid-induced pain mouse model	Analgesic, 5.0 mg/kg	-	-
48	Acetic acid-induced pain mouse model	Analgesic, 5.0 mg/kg	-	-
49	Acetic acid-induced pain mouse model	Analgesic, 5.0 mg/kg	-	-
50	Acetic acid-induced pain mouse model	Analgesic, 5.0 mg/kg	-	-
51	Acetic acid-induced pain mouse model	Analgesic, 5.0 mg/kg	-	-
52	Acetic acid-induced pain mouse model	Analgesic, 1.0 mg/kg	-	-
53	Acetic acid-induced pain mouse model	Analgesic, 5.0 mg/kg	-	-
54	Acetic acid-induced pain mouse model	Analgesic, 5.0 mg/kg	-	-
55	Acetic acid-induced pain mouse model	Analgesic, 5.0 mg/kg	-	-
56	Acetic acid-induced pain mouse model	Analgesic, 0.04 mg/kg	-	-
57	Acetic acid-induced pain mouse model	Analgesic, 5.0 mg/kg	-	-
58	Acetic acid-induced pain mouse model	Analgesic, 5.0 mg/kg	-	-
59	Acetic acid-induced pain mouse model	Analgesic, 0.2 mg/kg	-	-
60	Acetic acid-induced pain mouse model	Analgesic, 5.0 mg/kg	-	-
61	Acetic acid-induced pain mouse model	Analgesic, 5.0 mg/kg	-	-
62	Acetic acid-induced pain mouse model	Analgesic, 5.0 mg/kg	-	-

Table 2. Cont.

No	In Vivo		In Vitro	
	Test Mode	Activity/Dose	Test Model	Activity/Dose
63	Acetic acid-induced pain mouse model	Analgesic, 5.0 mg/kg	-	
64	Acetic acid-induced pain mouse model	Analgesic, 5.0 mg/kg	-	
65	Acetic acid-induced pain mouse model	Analgesic, 5.0 mg/kg	-	
66	Acetic acid-induced pain mouse model	Analgesic, 5.0 mg/kg	-	
67	Acetic acid-induced pain mouse model	Analgesic, 5.0 mg/kg	-	
68	Acetic acid-induced pain mouse model	Analgesic, 20.0 mg/kg	-	
69	Acetic acid-induced pain mouse model	Analgesic, 20.0 mg/kg	-	
70	-		-	
71	Acetic acid-induced pain mouse model	Analgesic, 2.0 mg/kg	-	
72	-		-	
73	-		-	
74	Acetic acid-induced pain mouse model	Analgesic, 5.0 mg/kg	-	
75	Acetic acid-induced pain mouse model	Analgesic, 0.04 mg/kg	-	
76	Acetic acid-induced pain mouse model	Analgesic, 0.04 mg/kg	-	
77	Acetic acid-induced pain mouse model	Analgesic, 5.0 mg/kg	-	
78	Acetic acid-induced pain mouse model	Analgesic, 5.0 mg/kg	-	
79	Acetic acid-induced pain mouse model	ND	-	
80	Acetic acid-induced pain mouse model	Analgesic, 5.0 mg/kg	-	
81	Acetic acid-induced pain mouse model	Analgesic, 5.0 mg/kg	-	
82	-		-	
83	Acetic acid-induced pain mouse model	Analgesic, 5.0 mg/kg	-	
84	-		Anti-inflammatory	ND, 10 µg/mL
85	-		Anti-inflammatory	10 µg/mL
86	-		Anti-inflammatory	10 µg/mL
87	Acetic acid-induced pain mouse model	Analgesic, 5.0 mg/kg	-	
88	Acetic acid-induced pain mouse model	Analgesic, 5.0 mg/kg	-	
89	Acetic acid-induced pain mouse model	Analgesic, 5.0 mg/kg	-	
90	Acetic acid-induced pain mouse model	Analgesic, 5.0 mg/kg	-	
91	Acetic acid-induced pain mouse model	Analgesic, 5.0 mg/kg	-	
92	Acetic acid-induced pain mouse model	Analgesic, 5.0 mg/kg	-	
93	Acetic acid-induced pain mouse model	Analgesic, 1.0 mg/kg	-	
94	Acetic acid-induced pain mouse model	Analgesic, 0.8 mg/kg	-	
95	-		-	
96	-		-	
97	-		-	
98	-		Anti-inflammatory	ND, 40 µM
99	-		Anti-inflammatory	ND, 40 µM
100	-		Anti-inflammatory	IC ₅₀ 35.4 ± 3.9 µM
101	-		Anti-inflammatory	ND, 40 µM
102	-		Anti-inflammatory	ND, 40 µM
103	Acetic acid-induced pain mouse model	Analgesic, 10.0 mg/kg	-	
104	-		-	
105	Acetic acid-induced pain mouse model	Analgesic, 5.0 mg/kg	-	
106	Acetic acid-induced pain mouse model	Analgesic, 5.0 mg/kg	-	

Table 2. Cont.

No	In Vivo		In Vitro	
	Test Mode	Activity/Dose	Test Model	Activity/Dose
107	Acetic acid-induced pain mouse model	Analgesic, 5.0 mg/kg	-	
108	-		-	
109	Acetic acid-induced pain mouse model	Analgesic, 5.0 mg/kg	-	
110	Acetic acid-induced pain mouse model	Analgesic, 5.0 mg/kg	-	
111	Acetic acid-induced pain mouse model	Analgesic, 5.0 mg/kg	-	
112	Acetic acid-induced pain mouse model	Analgesic, 5.0 mg/kg	-	
113	Acetic acid-induced pain mouse model	Analgesic, 5.0 mg/kg	-	
114	Acetic acid-induced pain mouse model	Analgesic, 20.0 mg/kg	-	
115	Acetic acid-induced pain mouse model	Analgesic, 5.0 mg/kg	-	
116	Acetic acid-induced pain mouse model	Analgesic, 5.0 mg/kg	-	
117	Acetic acid-induced pain mouse model	Analgesic, 0.2 mg/kg	-	
118	Acetic acid-induced pain mouse model	Analgesic, 5.0 mg/kg	-	
119	Acetic acid-induced pain mouse model	Analgesic, 5.0 mg/kg	-	
120	Acetic acid-induced pain mouse model	Analgesic, 5.0 mg/kg	-	
121	Acetic acid-induced pain mouse model	Analgesic, 5.0 mg/kg	-	
122	Acetic acid-induced pain mouse model	Analgesic, 0.2 mg/kg	-	
123	-		Anti-inflammatory	ND, 10 µg/mL
124	-		Anti-inflammatory	ND, 10 µg/mL
125	-		Anti-inflammatory	10 µg/mL
126	Acetic acid-induced pain mouse model	Analgesic, 5.0 mg/kg	-	
127	Acetic acid-induced pain mouse model	Analgesic, 5.0 mg/kg	-	
128	Acetic acid-induced pain mouse model	Analgesic, 5.0 mg/kg	-	
129	Acetic acid-induced pain mouse model	Analgesic, 5.0 mg/kg	-	
130	Acetic acid-induced pain mouse model	Analgesic, 5.0 mg/kg	-	
131	Acetic acid-induced pain mouse model	Analgesic, 0.2 mg/kg	-	
132	Acetic acid-induced pain mouse model	Analgesic, 5.0 mg/kg	-	
133	Acetic acid-induced pain mouse model	Analgesic, 5.0 mg/kg	-	
134	Acetic acid-induced pain mouse model	Analgesic, 1.0 mg/kg	-	
135	Acetic acid-induced pain mouse model	Analgesic, 1.0 mg/kg	-	
136	Acetic acid-induced pain mouse model	Analgesic, 1.0 mg/kg	-	
137	Acetic acid-induced pain mouse model	Analgesic, 0.04 mg/kg	-	
138	Acetic acid-induced pain mouse model	Analgesic, 5.0 mg/kg	-	
139	Acetic acid-induced pain mouse model	Analgesic, 5.0 mg/kg	-	
140	Acetic acid-induced pain mouse model	Analgesic, 5.0 mg/kg	-	
141	Acetic acid-induced pain mouse model	Analgesic, 5.0 mg/kg	-	
142	Acetic acid-induced pain mouse model	Analgesic, 5.0 mg/kg	-	
143	-		-	
144	-		-	
145	-		Anti-inflammatory	ND, 40 µM
146	-		-	
147	Acetic acid-induced pain mouse model	Analgesic, 5.0 mg/kg	-	
148	Acetic acid-induced pain mouse model Capsaicin-induced pain mouse model AITC-induced pain mouse model	Analgesic, 0.2 mg/kg Analgesic, 5.0 mg/kg Analgesic, 5.0 mg/kg	-	

Table 2. Cont.

No	In Vivo		In Vitro	
	Test Mode	Activity/Dose	Test Model	Activity/Dose
149	Acetic acid-induced pain mouse model	Analgesic, 5.0 mg/kg		
150	Acetic acid-induced pain mouse model	Analgesic, 10.0 mg/kg	-	
151	-		-	
152	Acetic acid-induced pain mouse model	Analgesic, 10.0 mg/kg	-	
153	Acetic acid-induced pain mouse model	Analgesic, 5.0 mg/kg	-	
154	Acetic acid-induced pain mouse model	Analgesic, 5.0 mg/kg	-	
155	Acetic acid-induced pain mouse model	Analgesic, 1.0 mg/kg	-	
156	Acetic acid-induced pain mouse model	Analgesic, 1.0 mg/kg	-	
157	Acetic acid-induced pain mouse model	Analgesic, 1.0 mg/kg	-	
158	-		-	
159	Acetic acid-induced pain mouse model	Analgesic, 5.0 mg/kg	-	
160	Acetic acid-induced pain mouse model	Analgesic, 5.0 mg/kg	-	
161	Acetic acid-induced pain mouse model	Analgesic, 5 mg/kg Antifeedant, 0.5 mg/mL	-	
162	Acetic acid-induced pain mouse model	Analgesic, 1.0 mg/kg	-	
163	Acetic acid-induced pain mouse model	Analgesic, 5.0 mg/kg	-	
164	Acetic acid-induced pain mouse model	Analgesic, 5.0 mg/kg	-	
165	-		-	
166	Acetic acid-induced pain mouse model	Analgesic, 5.0 mg/kg	-	
167	<i>Plutella xylostella</i>	Antifeedant, 0.5 mg/mL	-	
168	-		-	
169	Acetic acid-induced pain mouse model	Analgesic, 1.0 mg/kg	-	
170	Acetic acid-induced pain mouse model	Analgesic, 1.0 mg/kg	-	
171	Acetic acid-induced pain mouse model	Analgesic, 5.0 mg/kg	-	
172	Acetic acid-induced pain mouse model	Analgesic, 5.0 mg/kg	-	
173	Acetic acid-induced pain mouse model	Analgesic, 1.0 mg/kg	-	
174	Acetic acid-induced pain mouse model	Analgesic, 5.0 mg/kg	-	
175	Acetic acid-induced pain mouse model	Analgesic, 1.0 mg/kg	-	
176	Acetic acid-induced pain mouse model	Analgesic, 5.0 mg/kg	-	
177	Acetic acid-induced pain mouse model	Analgesic, 0.04 mg/kg	-	
178	Acetic acid-induced pain mouse model	Analgesic, 0.2 mg/kg	-	
179	Acetic acid-induced pain mouse model	Analgesic, 1.0 mg/kg	-	
180	-		-	
181	Acetic acid-induced pain mouse model	Analgesic, 5.0 mg/kg	-	
182	-		PTP1B	IC ₅₀ 22.99 ± 0.43 μM
183	-		PTP1B	IC ₅₀ 32.24 ± 0.74 μM
184	Acetic acid-induced pain mouse model	Analgesic, 10.0 mg/kg	-	
185	-		-	
186	Acetic acid-induced pain mouse model	Analgesic, 1.0 mg/kg	-	
187	Acetic acid-induced pain mouse model	Analgesic, 1.0 mg/kg	-	
188	Acetic acid-induced pain mouse model	Analgesic, 5.0 mg/kg	-	
189	Acetic acid-induced pain mouse model	Analgesic, 5.0 mg/kg	-	
190	Acetic acid-induced pain mouse model	Analgesic, 5.0 mg/kg	-	

Table 2. Cont.

No	In Vivo		In Vitro	
	Test Mode	Activity/Dose	Test Model	Activity/Dose
191	Acetic acid-induced pain mouse model	Analgesic, 5.0 mg/kg	-	
192	-		-	
193	Acetic acid-induced pain mouse model	Analgesic, 0.2 mg/kg	-	

ND: Inactive at the tested concentration; -: Did not test.

2.1. Normal Grayanane-Type Diterpenes (1–97)

Normal grayanane diterpenes, a predominant class of diterpenes, have been the subject of extensive research, culminating in the discovery of 97 unique compounds. Characterized by their distinctive 5/7/6/5 tetracyclic framework, these compounds are depicted in Figures 2–4 and elaborated upon in Tables 1 and 2. This section meticulously explores the remarkable identification of these 97 novel grayanane diterpenes, each marked by a unique tetracyclic structure comprising four interconnected carbon rings. Notably, the grayanane diterpenes display a standard 5/7/6/5 configuration within their tetracyclic systems, a configuration that sets them apart from other diterpene structures. This divergence often translates into varied biological properties and potential applications, underscoring the significance of this discovery.

Pierisformosoids A–L (1–12) were isolated and identified from the roots of *Pieris formosa* [10]. Notably, compounds 1, 2, 4–5, and 7–8 demonstrated significant analgesic activity in an acetic acid-induced writhing test in mice at a dosage of 5.0 mg/kg (i.p.), with compound 7 being five times more potent than positive control morphine. Compounds 1, 4, and 9 showed antifeedant activity against *Plutella xylostella* at 0.5 mg/mL. Compound 4 inhibited the KCNQ2 potassium channel by 38.3% at a concentration of 10 mM. Thirteen novel grayanane diterpenes (13–25) were isolated from the leaves of *R. micranthum*, and the structures were identified through extensive spectroscopic analysis and X-ray diffraction [11]. Compound 13 is notable as the first example of a 3 α -oxygrayanane diterpenoid glucoside. Compounds 14–17 are the first examples of 5 α -hydroxy-1- β H-grayanane diterpenoids, and compounds 16–18 and 20–21 represent the first grayanane glucosides with glucosylation at C-16. Compounds 14, 15, 19–22, and 24–25 exhibited significant antinociceptive effects at 5 mg/kg, surpassing 50% inhibition using morphine as a positive control in the acetic acid-induced writhing test. Zhou et al. reported eight novel diterpenes compounds (26–33) from the leaves of *R. molle* [9]. Additionally, Zhu et al. identified seven new diterpenes (34–39) from the leaves and twigs of *R. decorum* [25], with compounds 34, and 36–39 displaying significant antinociceptive activity at 10 mg/kg. Compound 38 was particularly potent, inhibiting 68.0% writhes at a dose of 0.8 mg/kg.

Five analgesic grayanane diterpene glucosides, 40 [24] and 41–44 [17], were isolated and illustrated from leaves of *R. auriculatum* and *R. micranthum*, respectively. At a dose of 1.0 mg/kg, compound 40 displayed notable analgesic activity with the acetic acid-induced writhing test. Compound 43 significantly reduced the number of writhes with an inhibition rate of over 50% at the same dosage. Compounds 45–55, isolated by Sun et al. from the leaves of *R. auriculatum*, and their structures were defined via extensive spectroscopic data analysis and X-ray diffraction analysis [28]. Compound 45 represents the first example of a 3 α ,5 α -dihydroxy-1- β H-grayanane diterpenoid, while 49 and 50 are the first examples of 19-hydroxygrayanane and grayan-5(6)-ene diterpenoids, respectively. Compounds 45–55 all showed significant analgesic activities at 5.0 mg/kg in an acetic acid-induced writhing test with an inhibition rate over 50%. From a leaf extract of *P. japonica*, twelve novel antinociceptive grayanane diterpenoids, 56–67, were isolated and determined by spectroscopic methods as well as X-ray diffraction analysis [29]. Compound 56 represents the first example of a 17-hydroxygrayan-15(16)-ene diterpenoid and exhibited potent antinociceptive effects with writhe inhibition rates of 56.3% and 64.8% at doses of

0.04 and 0.2 mg/kg, respectively, with effects comparable to the positive control morphine in the HOAc-induced writhing test in mice.

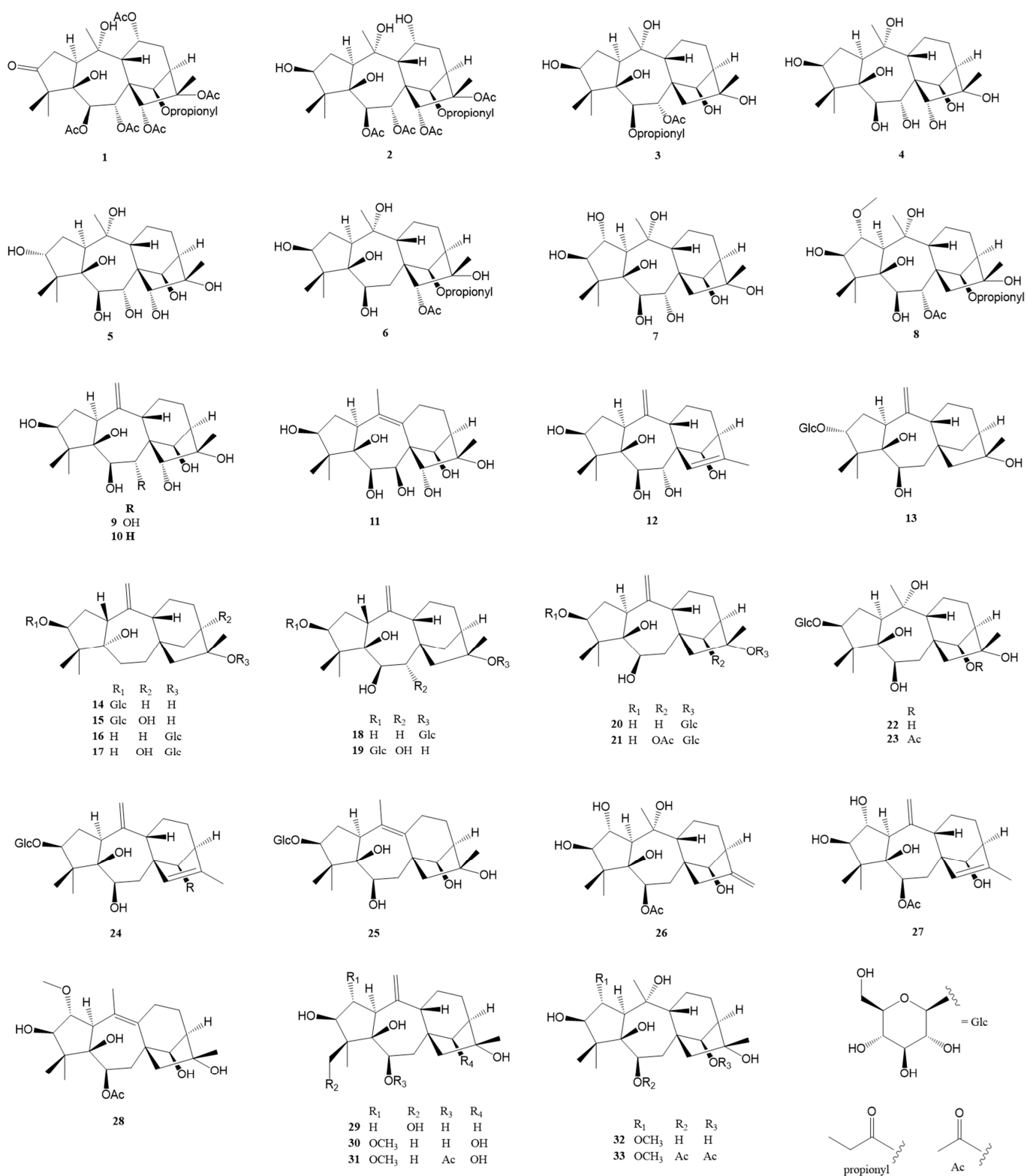


Figure 2. Structures of compounds 1–33.

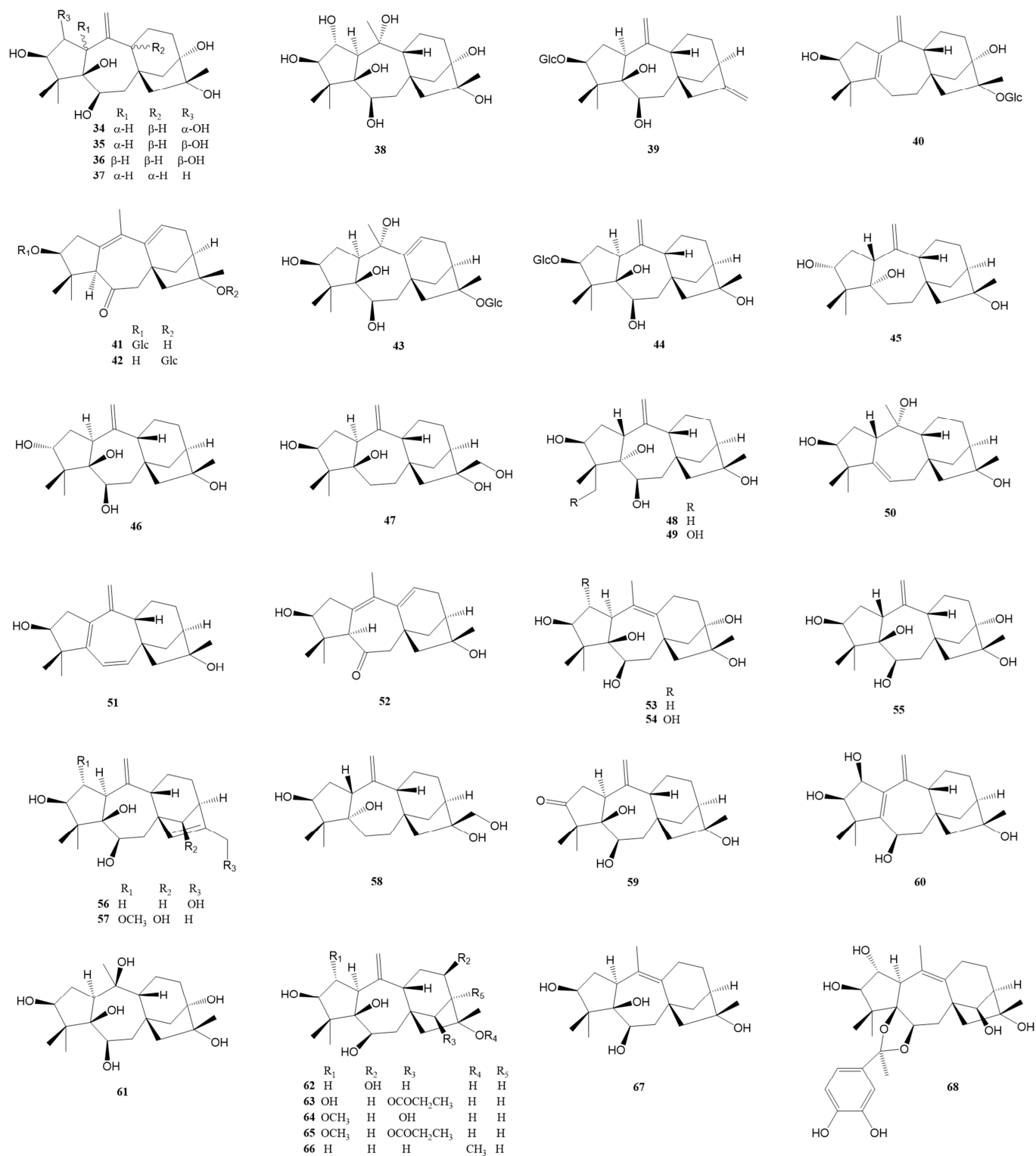


Figure 3. Structures of compounds 34–68.

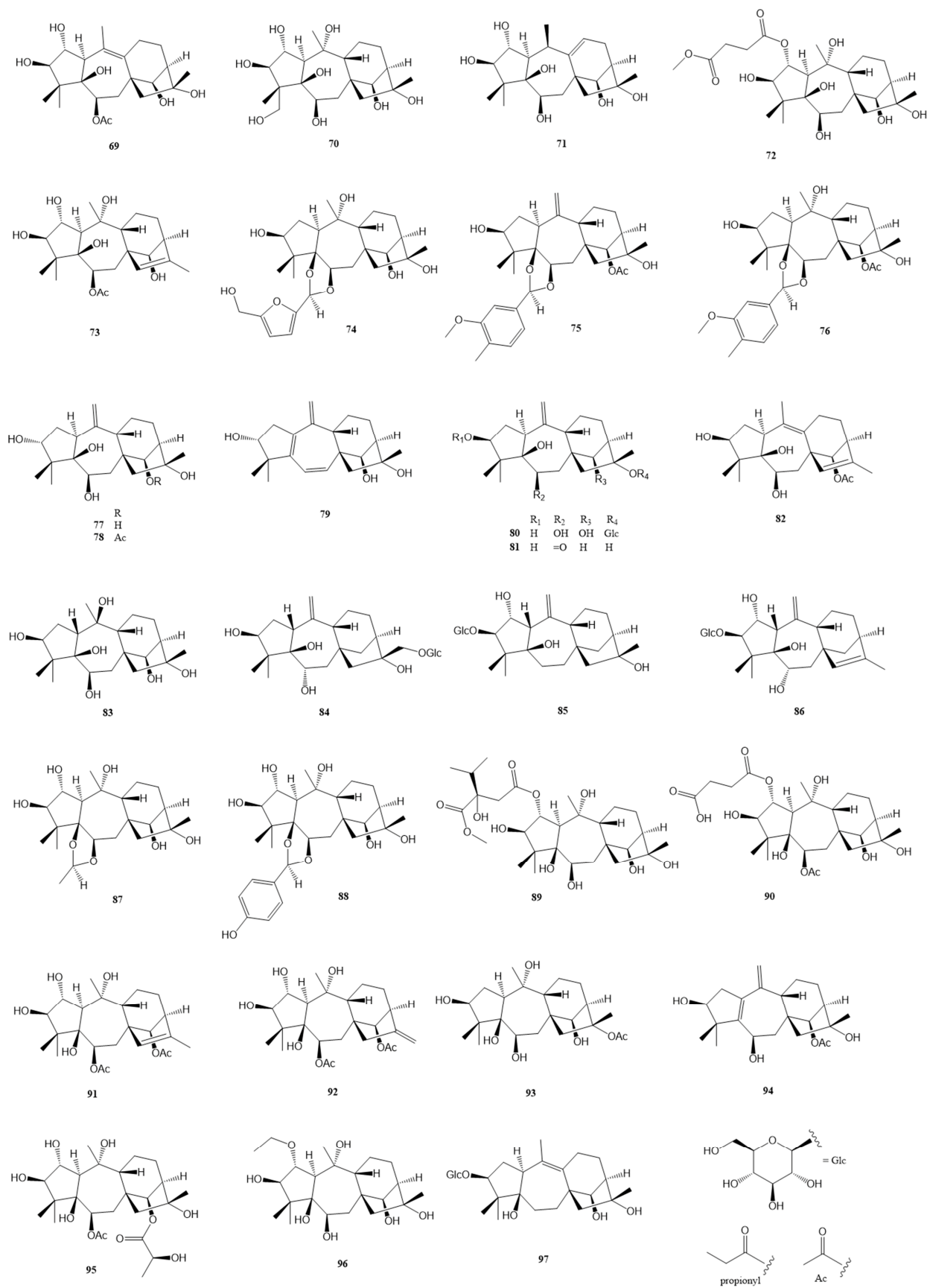


Figure 4. Structures of compounds 69–97.

Li et al. reported six novel grayanane diterpenes (68–73) from the flowers of *R. molle* [23], with compound 71 inhibiting 46.0% of acetic acid-induced writhes at a dose of 2.0 mg/kg. Three 1,3-dioxolane conjugates of grayanane diterpenoids (74–76) with 5-hydroxymethylfurfural and vanillin, respectively, were isolated from the flowers of *R. dauricum* [19]. The structures were determined by spectroscopic methods and confirmed by X-ray diffraction analysis. At a lower dose of 0.04 mg/kg, 75 and 76 exhibited more potent activity than morphine in efficacy with inhibition rates of 62.8% and 53.2%, respectively. In chemical investigation of the flowers of *R. dauricum*, seven highly oxygenated grayanane diterpenes (77–83) were discovered [30], with compound 79 being a notable conjugated grayan-1(5),6(7),9(10)-triene diterpenoid. Among compounds 84–86, purified from the leaves of *C. yunnanense* [31], 84 and 85 displayed significant anti-inflammatory activity, particularly inhibiting IL-6 release in lipopolysaccharide (LPS)-induced RAW264.7 cells. Zheng et al. identified six new diterpenes (87–92) from the flowers of *R. molle* as potent analgesics [32]. Notably, compound 92 demonstrated remarkable activity, remaining effective even at the dose of 0.04 mg/kg in vivo pain assay screenings. Chai et al. discovered compounds 93 and 94 from the roots of *R. micranthum* [22], both showing strong antinociceptive effects at doses of 0.1 mg/kg and 0.8 mg/kg, respectively. More recently, three additional minor grayanane diterpenes (95–97) were isolated and elucidated from the leaves of *C. yunnanense* [33].

2.2. Epoxy-Grayanane (98–132)- and Seco-Grayanane (133–142)-Type Diterpenes

Epoxy-grayanane diterpenes represent a unique subset within the larger grayanane family, distinguished primarily by their epoxy group moiety. These compounds, numbering thirty-five in total, are defined by the inclusion of one or two epoxy groups in their structure. The positioning of these epoxy groups varies, occurring between different sets of carbon atoms. This variation leads to a range of configurations, such as C2-C3, C6-C10, C7-C10, C5-C9, C9-C10, C5-C20, C11-C16, and even combinations like C2-C3 with C9-C10, and C2-C3 with C11-C16. These configurations are detailed in Figures 5 and 6 and Table 1.

In addition, there is a category known as *seco*-grayanane diterpenes, of which eight varieties have been identified. These compounds are marked by a distinct feature: a structural ring opening, which results in different types, including 1,5-*seco*-grayanane, 1,10-*seco*-grayanane, and 1,10:2,3-*diseco*-grayanane. These are illustrated in Figure 6 and also listed in Table S1. The diversity in the structure of these diterpenes, particularly the placement and number of epoxy groups, contributes to their unique chemical properties and potential applications. The existence of both epoxy-grayanane and *seco*-grayanane diterpenes within the grayanane family highlights the complexity and variety inherent in natural compounds. The detailed categorization and identification of these compounds, as shown in the figures and tables, provide a valuable framework for further research and understanding of their characteristics and uses.

Zhou et al. reported the isolation of five epoxy-grayanane diterpenes (98–102) from *R. molle* [9]. Notably, compound 98 represents the first example of a 2,3:11,16-diepoxo grayanane diterpenoid, showcasing a unique cis/trans/cis/cis/trans-fused 3/5/7/6/5/5 hexacyclic ring system with a 7,13-dioxahexacyclo-[10.3.3.0^{1,11}.0^{4,9}.0^{6,8}.0^{14,17}]octadecane scaffold. The structure was confirmed through X-ray diffraction analysis. Compound 100 exhibited significant anti-inflammatory activity in LPS-stimulated RAW264.7 mouse macrophages with an IC₅₀ at 35.4 ± 3.9 μM. Two additional epoxy-grayanane diterpenes (103–104) were reported with a hydroxy group replaced at C-13 [25]. At 10.0 mg/kg, compound 103 displayed a mild antinociceptive effect. Furthermore, diverse epoxy-grayanane diterpenes (105–112) with analgesic activity were isolated from the roots of *P. formosa* [34]. Compounds 105–109 represent the first example of natural grayanane diterpenoids possessing a 10,14-epoxy group, while compounds 110–111 are the first example of grayanane diterpenoids possessing a 7,10-epoxy group. Compounds 105–107 and 109–112 showed significant analgesic activity at a dose of 5.0 mg/kg (i.p.) in the acetic acid-induced writhing test, with ibuprofen and morphine as the positive controls.

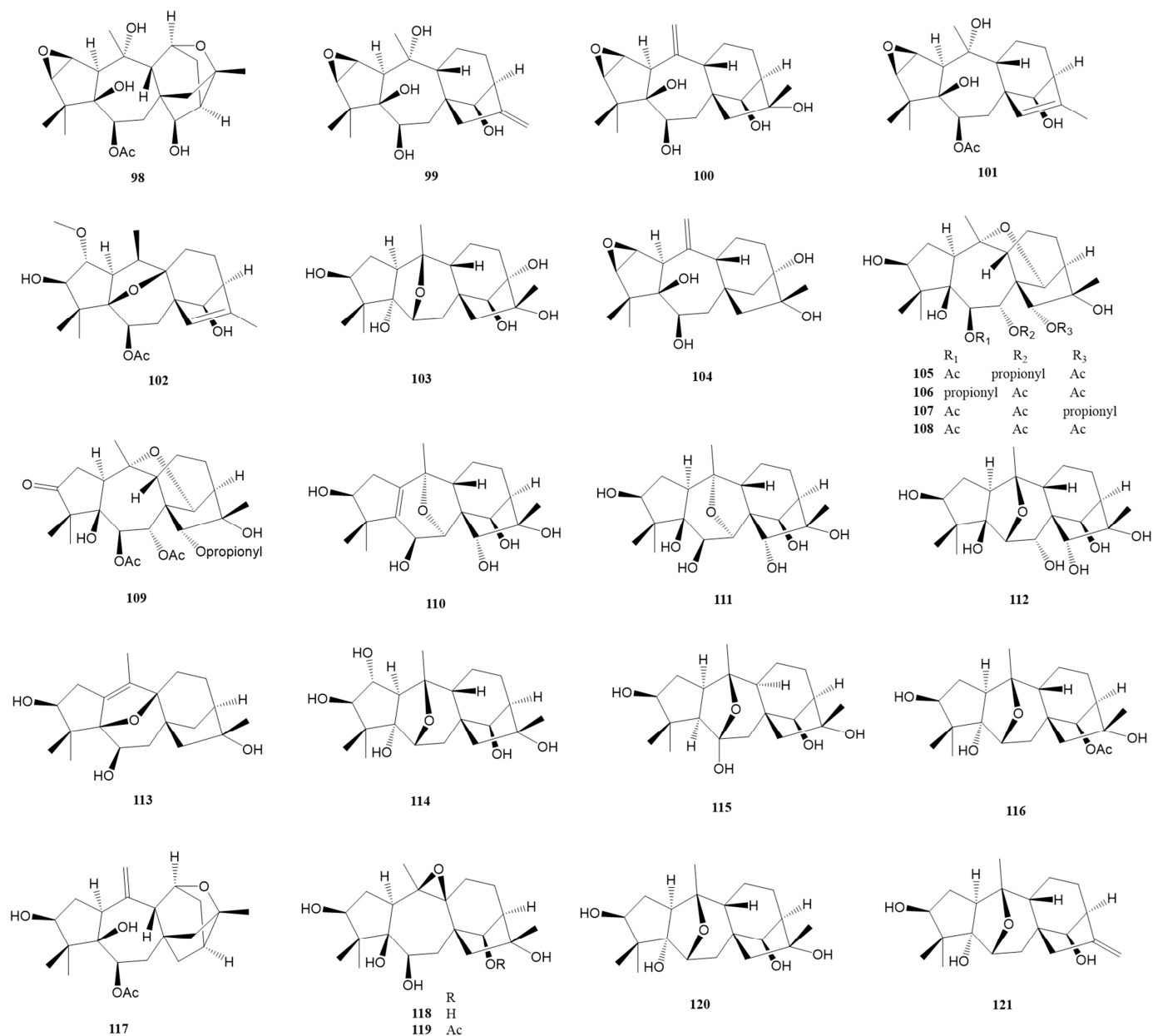


Figure 5. Structures of compounds 98–121.

Compound **113**, the second example of a $5\beta,9\beta$ -epoxygrayan-1(10)-ene diterpenoid, exhibited noticeable antinociceptive activity at 5.0 mg/kg in the acetic acid-induced writhing test in mice [29]. Three 6,10-epoxy grayanane diterpenes (**114** [23] and **115–116** [20]) were reported from *R. molle* and *R. micranthum*, respectively. Compound **115** represents the first example of a $5\alpha H,9\alpha H$ -grayanane diterpenoid and a 6-hydroxy-6,10-epoxy grayanane diterpenoid. Compounds **117–122** with diverse epoxy groups were isolated from the flowers of *R. dauricum* [30]. Compound **117** is the first example of an 11,16-epoxygrayan-6-one diterpenoid, while compounds **118** and **119** are the first examples of $9\beta,10\beta$ -epoxy grayanane diterpenoids. All these compounds (**117–122**) displayed significant analgesic activity in the acetic acid-induced writhing test in mice at 5.0 mg/kg, with inhibition rates over 50%. Compounds **117** and **122** were particularly potent, showing notable analgesic activity even at a lower dose of 0.2 mg/kg, with inhibition rates of 54.4% and 55.2%, respectively. Li et al. reported three undescribed epoxy-grayanane diterpenes (**123–125**) from *C. yunnanense*, with compound **125** notably inhibiting pro-inflammatory cytokines IL-6 at 10 $\mu\text{g/mL}$ [31]. Six highly functionalized epoxy diterpenes (**126–131**) were elucidated

by Zheng et al. from the flowers of *R. molle* [32]. Compounds **126**, **127**, and **130** are the first representatives of 2 β ,3 β :9 β ,10 β -diepoxygrayanane, 2,3-epoxygrayan-9(11)-ene, and 5,9-epoxygrayan-1(10),2(3)-diene diterpenoids, respectively. Compound **131** exhibited an inhibition rate of 51.4%, showing a more potent analgesic effect than morphine at a lower dose of 0.2 mg/kg in the acetic acid-induced writhing model. Compound **132** is another grayanane diterpene featuring a 5,20-epoxy group [28].

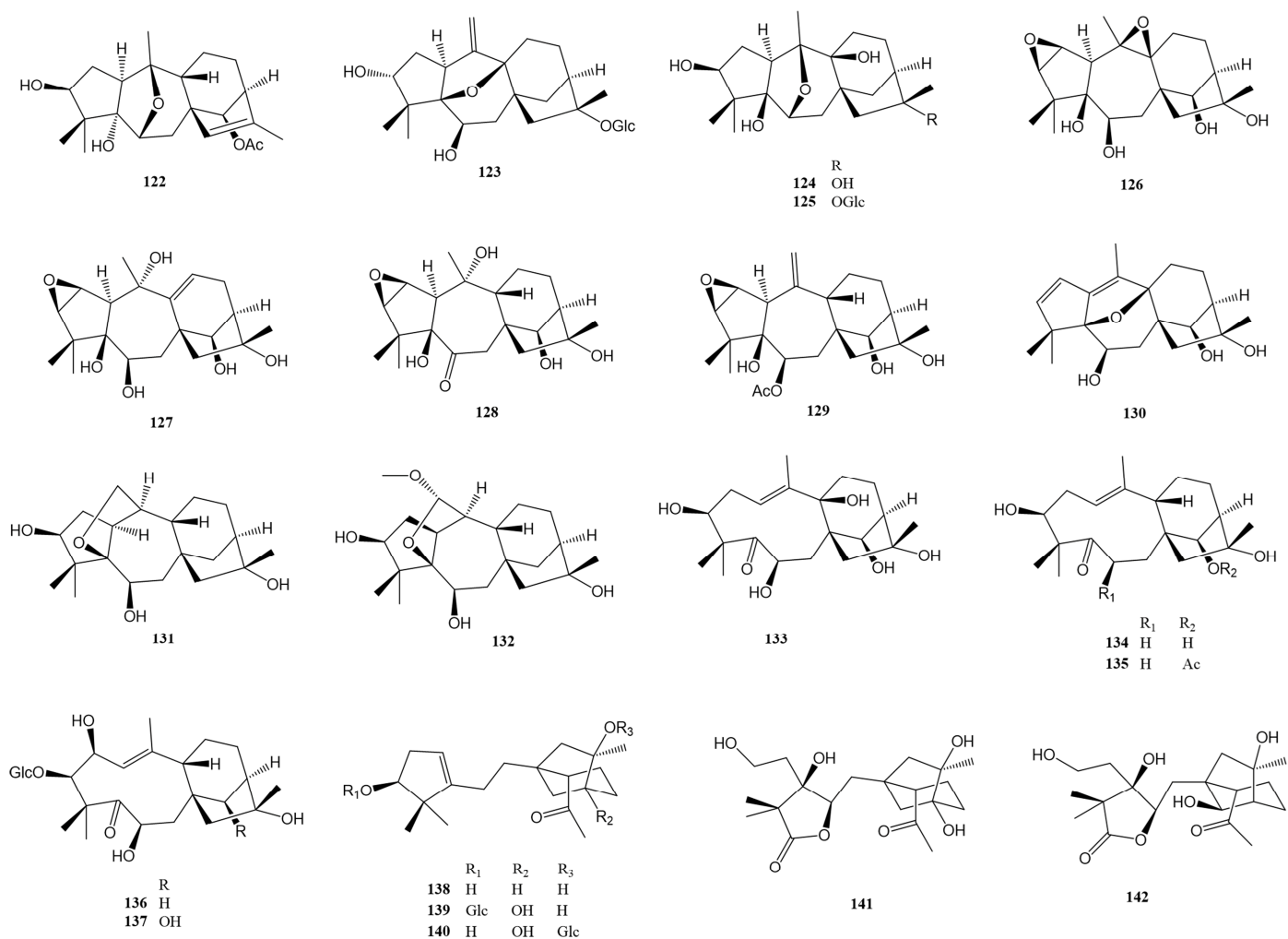


Figure 6. Structures of compounds **122–142**.

Compounds **133** [20] and **134–135** [19], displaying a 1,5-*seco*-grayanane carbon skeleton, were identified from *R. micranthum* and *R. dauricum*, respectively. Significantly, compounds **134** and **135** represent the first examples of 6-deoxy-1,5-*seco*-grayanane diterpenoids. Compounds **136–137** are distinguished as the first 1,5-*seco*-grayanane diterpenoid glucosides. Interestingly, these compounds exhibited only 17 carbon resonances instead of 26 carbons in their ¹³C NMR spectra. Their structures were conclusively determined by single-crystal X-ray diffraction [21]. The rare 1,10-*seco*-grayanane diterpenes, compounds **138–140**, were identified from the extracts of the leaves of *R. auriculatum*. Their structures were elucidated using NMR and ECD data analysis and were further confirmed by X-ray diffraction [24]. Additionally, two 1,10:2,3-*diseco*-grayanane diterpenes, compounds **141** [24] and **142** [21], were successfully reported. The primary difference between these two compounds is the absence of the OH-13 group in compound **142**.

2.3. Grayanane Dimers-Type Diterpenes (143–149)

In the referenced scientific literature, there is a notable report detailing the discovery of seven unique grayanane dimer diterpenes. This significant finding is visually documented in Figure 7 and comprehensively listed in Table 1. These dimer compounds, which represent a unique and complex class of natural products, are characterized by their distinctive structural formation. Specifically, they are formed through the connection of two grayanane monomer units. This connection is achieved via one or two ether bonds, a type of chemical bond that involves an oxygen atom linked to two alkyl or aryl groups.

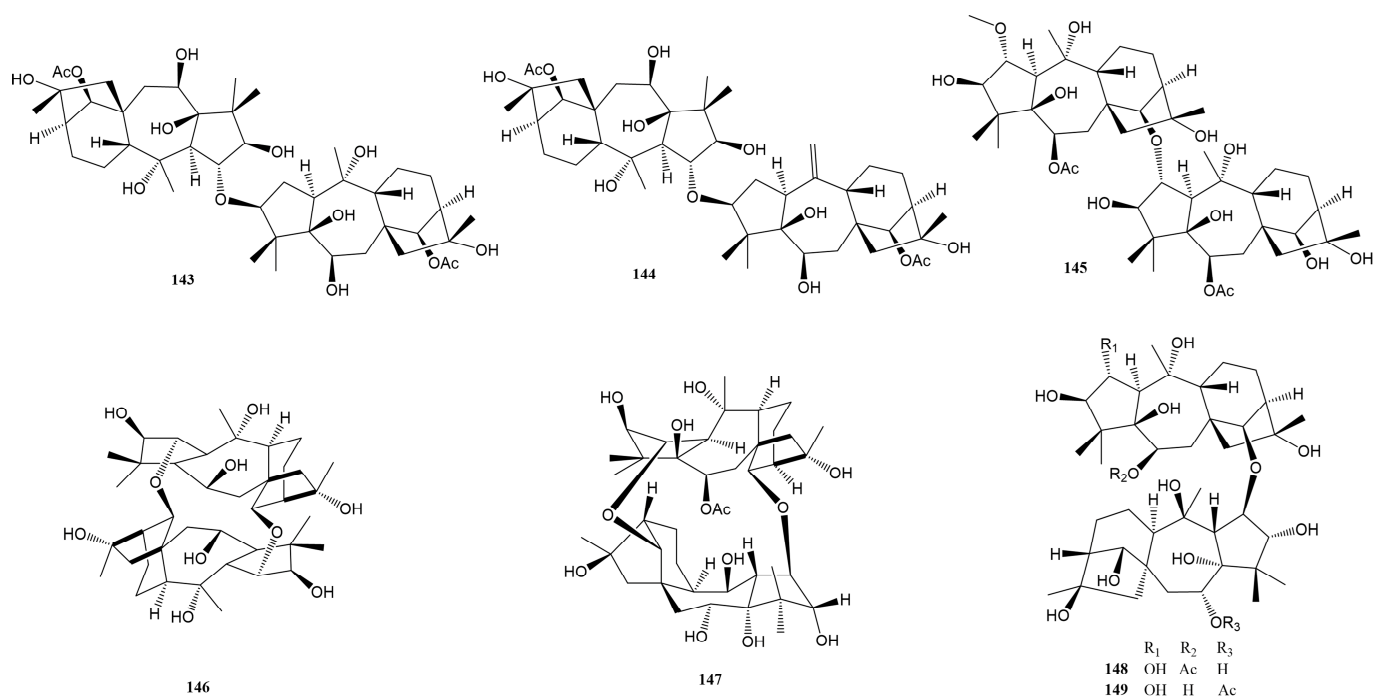


Figure 7. Structures of compounds 143–149.

Two new dimeric diterpenes (**143** and **144**) were characterized from the fruits of *R. pumilum*, representing the first examples of dimeric grayanane diterpenes with a 3-O-2' linkage from the Ericaceae family [35]. Another novel dimeric diterpene **145** [9] was identified from the leaves of *R. molle* but with a 13-O-2' linkage. Compound **146** is a unique dimeric grayanoid, isolated from the flowers of *R. molle* [23], containing a novel 14-membered heterocyclic ring with a C₂ symmetry axis. More recently, Huang et al. reported three new dimers, **147–149**, also from the flowers of *R. molle* [27]. The structures were determined by comprehensive spectroscopic data analysis, ¹³C NMR calculation with DP4+ analysis, and single-crystal X-ray diffraction analysis [27]. Of particular interest is compound **147**, a caged dimeric grayanane diterpenoid linked through two oxygen bridges of C-2–O–C-14' and C-14–O–C-2', featuring a unique 1,8-dioxacyclotetradecane motif. At a dose of 5.0 mg/kg, compounds **147–149** showed significant analgesic effects, with writhing inhibition rates exceeding 50% in the acetic acid-induced writhing test. Even at a lower dose of 1.0 mg/kg, compound **148** maintained an inhibition rate of 57.3%. Furthermore, in capsaicin- and AITC-induced pain models, compound **148** effectively reduced the nociceptive responses at a dose of 5.0 mg/kg, indicating its potential as a dual antagonist of TRPV1 and TRPA1.

2.4. Leucothane-Type Diterpenes (150–163)

Leucothane-type diterpenes represent a fascinating subset within the broader category of grayanane-type diterpenes, known for their unique biosynthetic relationships. These compounds are distinguished by their distinct structural framework, which features a

6/6/6/5 fused tetracyclic ring system. Over the past five years, there has been notable progress in the identification and characterization of these compounds. Fourteen new leucothane-type diterpenes have been discovered and reported, marking a significant advancement in the study of naturally occurring diterpenes. Details are shown in Figure 8 and Tables 1 and 2.

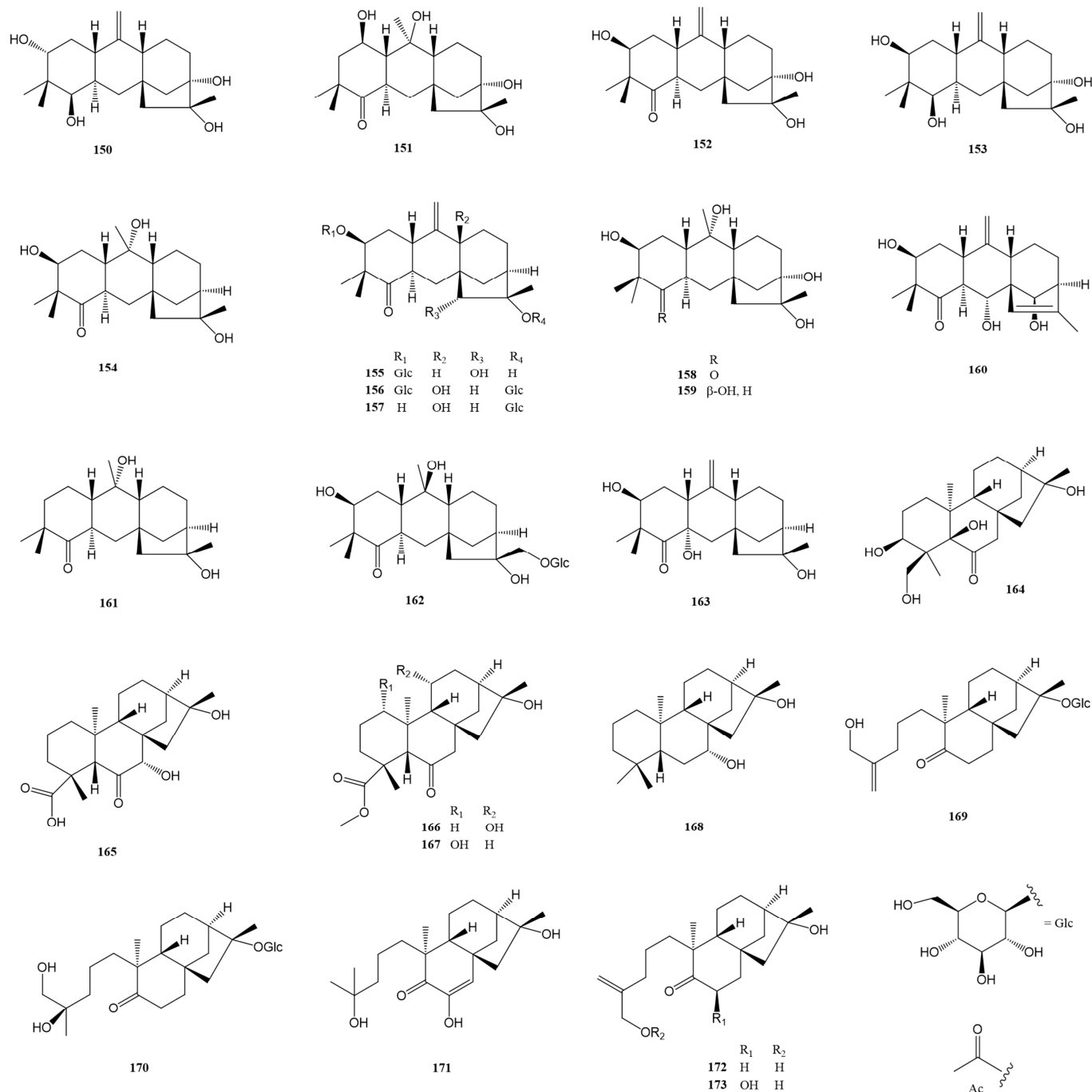


Figure 8. Structures of compounds 150–173.

Three new leucothane-type diterpenes (150–152) were isolated from the leaves and twigs of *R. decorum* [25]. The structure of compound 150 was confirmed by X-ray crystallography. In the acetic acid-induced writhing test, compound 150 showed a significant effect at a dose of 10.0 mg/kg. Sun et al. reported five new leucothane-type terpenes (153–154 [24] and 155–157 [17]) from *R. auriculatum* and *R. micranthum*, respectively. Compounds 155–157 represent the first examples of 15 α -hydroxy-leucothane diterpenoids, leucothane diterpene

diglucosides, and 9 β -hydroxy-leucothane diterpenoids, respectively. These compounds (153–157) all displayed potent analgesic activity in the acetic acid-induced writhing test. Four additional leucothane-type diterpenes (158–159 [23] and 160–161 [18]) were elucidated from *R. molle* and *P. formosa*, respectively. Compounds 159 and 160 demonstrated weak analgesic activity in the acetic acid-induced writhing test at 20.0 mg/kg and 5.0 mg/kg, respectively. In an antifeedant assay against *Plutella xylostella* larvae, compound 161 showed an inhibition effect with a ratio of 52.5% at a dose of 0.5 mg/mL. Lastly, two new leucothane-type diterpenes (162–163) were isolated and identified from *P. japonica* [21]. The structure of 163 was definitively confirmed through X-ray diffraction analysis. Notably, compound 162 exhibited strong analgesic activity with writhing inhibition over 50% at 5.0 mg/kg (i.p.).

2.5. Ent-Kaurane (164–168)- and Seco-Ent-Kaurane (169–173)-Type Diterpenes

Ent-kaurane-type diterpenes hold a crucial position in the biosynthesis of grayanane diterpenes, serving as bio-precursors in the intricate chemical pathways leading to the formation of grayanane structures. This role highlights the importance of understanding ent-kaurane-type diterpenes, not only for their inherent chemical properties but also for their contribution to the biosynthesis of other significant diterpenes. In the past five years, there has been a notable advancement in the research and identification of these compounds. Specifically, five ent-kaurane-type diterpenes and five 4,5-seco-ent-kaurane-type diterpenes have been successfully identified and reported. The 4,5-seco-ent-kaurane type represents a variation of the ent-kaurane structure, characterized by a unique opening in the ring structure, specifically between the 4th and 5th carbon atoms, which significantly alters their chemical and potentially biological properties. These discoveries are meticulously detailed in Figure 8 and Tables 1 and 2.

Sun et al. and Niu et al. successfully reported the new ent-kaurane-type diterpenes 164 [24] and 165–168 [18] from the leaves of *R. auriculatum* and the roots of *P. formosa*, respectively. A detailed analysis of the spectroscopic methods and ECD calculations illustrated the structures of these compounds. At 5.0 mg/kg, compounds 164 and 166 displayed weak analgesic activity in the acetic acid-induced writhing test. Compound 167 showed antifeedant activity against *Plutella xylostella* larvae with an inhibition ratio of 27.1% at 0.5 mg/mL. Additionally, five 4,5-seco-ent-kaurane-type diterpenes (169–170 [17], 171 [18], and 172–173 [21]) were successfully reported. Compounds 169–170, identified as diterpene glucosides at C-17, demonstrated potent analgesic effects at a 1.0 mg/kg dose in an acetic acid-induced writhing test.

2.6. Kalmane (174–179)- and Seco-Kalmane (180)-Type Diterpenes

Kalmane-type diterpenes stand out as a rare and intriguing class of terpenes that originate from the grayanane type. They are particularly renowned for their distinctive structural feature: a 5/8/5/5 fused tetracyclic ring system. This structure is not commonly found in terpenes, making the kalmane type a subject of significant interest in the study of natural products and organic chemistry. In the last five years, there has been substantial progress in identifying and reporting new kalmane-type diterpenes. Specifically, six kalmane-type diterpenes, 174 [20], 175–178 [36], 179 [22], and one 1,5-seco-kalmane-type 180 [23] have been reported, as illustrated in Figure 9 and Tables 1 and 2. Compound 175 is particularly noteworthy as it represents the first 5,8-epoxykalmane diterpenoid and the first kalm-15(16)-ene diterpenoid. Compounds 176–178 are the first examples of kalm-7(8)-ene, kalm-16(17)-ene, and 8 α -methoxykalmane diterpenoids, respectively. The structures of compounds 174–176 and 178 were undoubtedly elucidated via X-ray diffraction analysis. Regarding bioactivity, diterpenes 175–178 exhibited significant analgesic effects in an acetic acid-induced writhing test. Remarkably, compound 177 showed even more potent activity at a very low dose of 0.04 mg/kg.

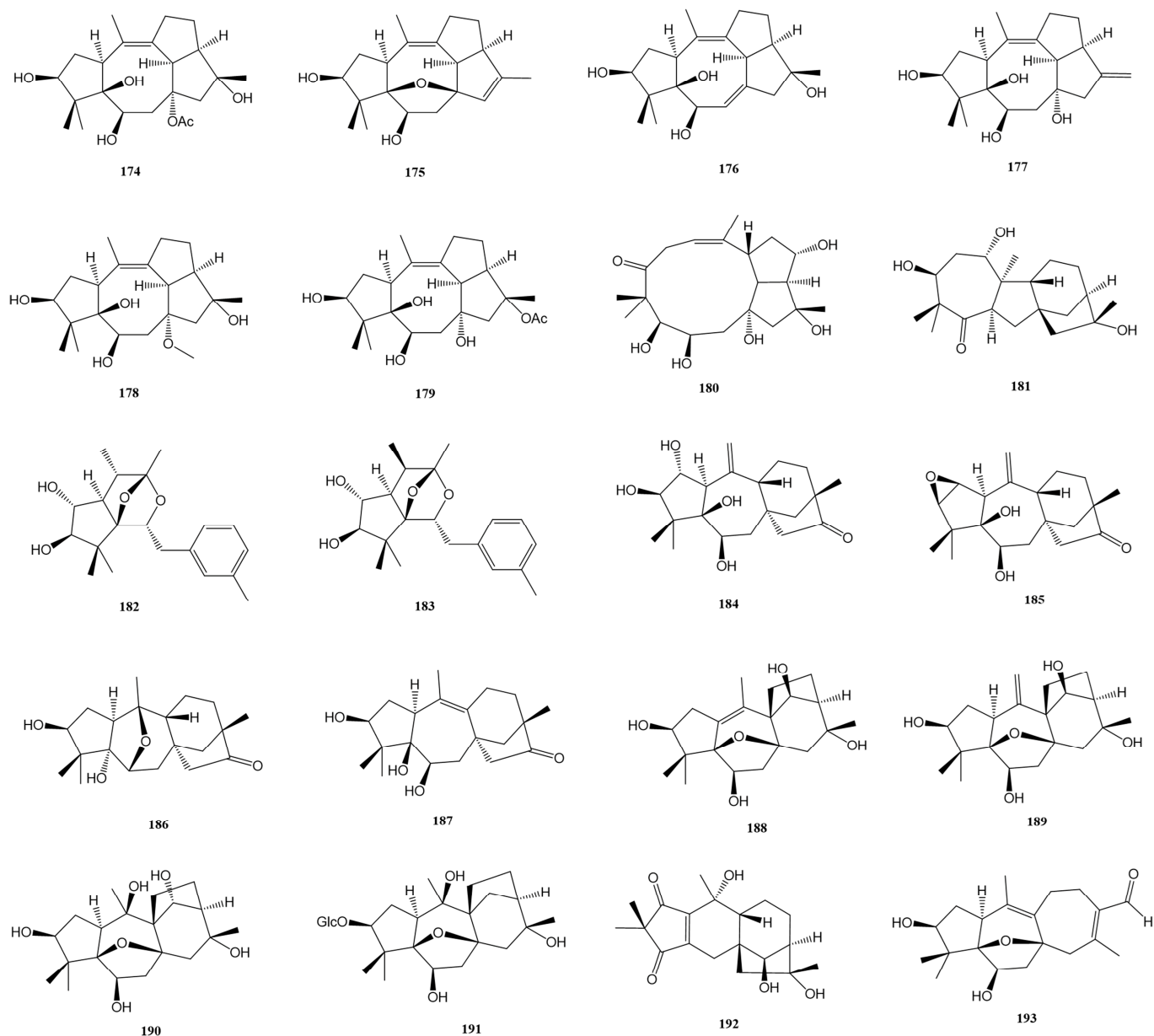


Figure 9. Structures of compounds 174–193.

2.7. Other Grayanane-Related Diterpenes (181–193)

This section focuses on a fascinating group of grayanane-related diterpenes characterized by their rare and rearranged carbon skeletons. These compounds, derived from various genera, showcase the remarkable diversity and complexity found in natural products, particularly in the realm of terpenoid chemistry. These compounds span a range of structural variations, including *A-home-B-nor-ent-kaurane* **181** [24], mollebenzylanes **182–183** [26], micranthanes **184–187** [20,25], molaranes **188–191** [20,21], rhomollane **192** [23], and rhodaruricane **193** [19], as shown in Figure 9 and Tables 1 and 2.

Compounds **182** and **183** are particularly notable for their unprecedented diterpene carbon skeleton, featuring a unique 9-benzyl-8,10-dioxatricyclo[5.2.1.0^{1,5}]decane core. The absolute structure of **182** was unambiguously determined via X-ray diffraction analysis of its *p*-bromobenzoate ester. Compound **186** is the first 6,10-epoxymicranthane, while compounds **188** and **189** represent the first examples of 14 β -hydroxymollane diterpenoids. Compound **191** is distinguished as the first mollane diterpene glucoside. Rhomollane **192** possesses an unprecedented 5/6/6/5 tetracyclic ring system (*B-nor* grayanane), incorporat-

ing a cyclopentene-1,3-dione scaffold. Its structure was undoubtedly solved by Mosher's method and X-ray diffraction of its Mosher ester. Rhodaruricane **193** features a unique 5/6/5/7 tetracyclic ring system with a 16-oxa-tetracyclo[11.2.1.0^{1,5}.0^{7,13}]hexadecane core. Quantum chemical calculations, including ¹³C NMR-DP4+ analysis ECD calculations, and single-crystal X-ray diffraction analysis, elucidated the absolute structure of **193**. In terms of biological activity, compounds **181**, **184**, and **185** showed significant antinociceptive activity in the acetic acid-induced writhing test at 5.0 mg/kg, with **184** maintaining significant activity even at 1.0 mg/kg. Compounds **182** and **183** exhibited moderate PTP1B inhibitory activities with IC₅₀ values of 22.99 ± 0.43 and 32.24 ± 0.74 μM, respectively.

3. Conclusions

Over the past five years, the field of phytochemistry has experienced a surge of progress, particularly in the study of grayanane diterpenes from the Ericaceae family. This period has been marked by the discovery of 193 novel diterpenes, each characterized by one of fifteen distinct carbon skeletons. This remarkable diversity not only underscores the richness of natural compounds but also highlights the ongoing potential for new and groundbreaking discoveries in this area. A significant focus of these studies has been on bioassay screenings, particularly evaluating *in vivo* pain activity using models like the acetic acid-induced writhing test. These tests have consistently demonstrated the potent analgesic properties of grayanane diterpenes. Additionally, certain compounds within this group have shown promising activity as inhibitors of PTP1B, suggesting potential therapeutic applications.

4. Future Perspectives

Looking to the future, the research into grayanane diterpenoids teems with exciting possibilities and opportunities. One critical area for future research is the detailed mechanistic study of these compounds, especially regarding their therapeutic applications [7]. Grayanane diterpenes are known for their potent toxicity, which is primarily attributed to their mechanism of action on the sodium channels in the nervous system, leading to a cascade of neurotoxic effects [7,37–39]. The limitations of using grayanane diterpenes stem from their narrow therapeutic index, the difficulty in controlling their dose-dependent toxic effects, and the potential for severe adverse reactions, including cardiac issues and central nervous system disturbances. Despite their potent bioactivity, which could be harnessed for therapeutic purposes, these limitations necessitate cautious handling and research to mitigate risks. Understanding the exact mode of action of grayanane diterpenes could revolutionize drug development and treatment strategies. This could lead to the creation of new drugs that harness the unique properties of these compounds, potentially offering more effective treatments for various conditions.

Another promising direction is the application of synthetic biology in the production of diterpenoids [40]. This approach could provide a sustainable and scalable alternative to traditional extraction methods from plants. This is particularly crucial for the large-scale production of these compounds, especially if they are to be used in therapeutic applications [41]. Synthetic biology might not only facilitate the production of these compounds but also enable the creation of novel diterpenoid derivatives with enhanced biological activities or reduced side effects.

Furthermore, exploring grayanane diterpenoids in combination therapies presents a significant opportunity for advancing medical treatments [42,43]. By combining these compounds with other drugs, there is potential to harness synergistic effects, which could lead to more effective treatments with fewer side effects. This approach aligns with the growing trend in pharmacology towards personalized medicine and treatment protocols that are more holistic and patient-specific. Moreover, exploring the broader range of biological activities of grayanane diterpenes is another avenue worth exploring. While much of the current research has focused on their analgesic and PTP1B inhibitory properties, these

compounds may have other biological activities that are yet to be discovered. Investigating these potential activities could open up new therapeutic areas for these compounds.

In terms of technological advancements, the development of more sophisticated analytical techniques will play a crucial role in future research [44–46]. Technological advances such as mass spectrometry, NMR spectroscopy, and X-ray crystallography could lead to more detailed and accurate structural elucidation of these compounds. This, in turn, would enhance our understanding of their chemical properties and biological activities. The potential for international collaboration in this field also presents an exciting opportunity. By bringing together researchers from different countries and disciplines, the study of grayanane diterpenes can benefit from a wide range of expertise and resources. Such collaborations could lead to more rapid advancements in the field and sharing knowledge and techniques across borders.

In summary, the study of grayanane diterpenes stands at a pivotal point, with numerous avenues for future research and potential applications in pharmaceuticals and therapeutics. The continued exploration of these natural compounds is poised to significantly contribute to our understanding of natural product chemistry, medicinal chemistry, and pharmacology. As research progresses, grayanane diterpenes will likely play an increasingly important role in the development of new drugs and treatment strategies, highlighting the importance of natural products in modern medicine.

Supplementary Materials: The following supporting information can be downloaded at: <https://www.mdpi.com/article/10.3390/molecules29071649/s1>, Table S1. Compound names, plant resources, related references, and published year; Table S2. Compound names and reported activities.

Author Contributions: S.L. and L.S., original draft preparation; P.Z., review and editing; C.N., conceptualization and supervision. All authors have read and agreed to the published version of the manuscript.

Funding: This report did not receive any funding.

Conflicts of Interest: The authors declare no conflicts of interest.

Abbreviations

AITC	Allyl isothiocyanate
LPS	lipopolysaccharide
NMR	Nuclear magnetic resonance
ECD	Electronic circular dichroism
PTP1B	Protein tyrosine phosphatase 1B
<i>C. yunnanense</i>	<i>Craibiodendron yunnanense</i>
<i>P. formosa</i>	<i>Pieris formosa</i>
<i>R. micranthum</i>	<i>Rhododendron micranthum</i>
<i>R. molle</i>	<i>Rhododendron molle</i>
<i>R. decorum</i>	<i>Rhododendron decorum</i>
<i>R. auriculatum</i>	<i>Rhododendron auriculatum</i>
<i>P. japonica</i>	<i>Pieris japonica</i>
<i>R. dauricum</i>	<i>Rhododendron dauricum</i>
<i>R. pumilum</i>	<i>Rhododendron pumilum</i>

References

1. Gershenzon, J.; Dudareva, N. The function of terpene natural products in the natural world. *Nat. Chem. Biol.* **2007**, *3*, 408–414. [[CrossRef](#)] [[PubMed](#)]
2. Li, Y.; Liu, Y.-B.; Yu, S.-S. Grayanoids from the Ericaceae family: Structures, biological activities and mechanism of action. *Phytochem. Rev.* **2013**, *12*, 305–325. [[CrossRef](#)]
3. Niu, C.-S.; Li, Y.; Liu, Y.-B.; Ma, S.-G.; Li, L.; Qu, J.; Yu, S.-S. Analgesic diterpenoids from the twigs of *Pieris formosa*. *Tetrahedron* **2016**, *72*, 44–49. [[CrossRef](#)]
4. Xiao, S.-M.; Niu, C.-S.; Li, Y.; Tang, Z.-S.; Qu, J. Chemical constituents from roots of *Pieris formosa* and their bioactivity. *Zhongguo Zhong Yao Za Zhi* **2018**, *43*, 964–969. [[PubMed](#)]

5. Niu, C.S.; Li, Y.; Liu, Y.B.; Ma, S.G.; Liu, F.; Li, L.; Xu, S.; Wang, X.J.; Wang, R.B.; Qu, J.; et al. Pierisketolide A and Pierisketones B and C, Three Diterpenes with an Unusual Carbon Skeleton from the Roots of *Pieris formosa*. *Org. Lett.* **2017**, *19*, 906–909. [[CrossRef](#)] [[PubMed](#)]
6. Liu, X.J.; Su, H.G.; Peng, X.R.; Bi, H.C.; Qiu, M.H. An updated review of the genus *Rhododendron* since 2010: Traditional uses, phytochemistry, and pharmacology. *Phytochemistry* **2024**, *217*, 113899. [[CrossRef](#)] [[PubMed](#)]
7. Yang, J.; Zhao, J.; Zhang, J. The efficacy and toxicity of grayanoids as analgesics: A systematic review. *J. Ethnopharmacol.* **2022**, *298*, 115581. [[CrossRef](#)] [[PubMed](#)]
8. Niu, C.-S.; Li, Y.; Liu, Y.-B.; Ma, S.-G.; Liu, F.; Li, L.; Xu, S.; Wang, X.-J.; Liu, S.; Wang, R.-B.; et al. Biological and chemical guided isolation of 3,4-secograyanane diterpenoids from the roots of *Pieris formosa*. *RSC Adv.* **2017**, *7*, 43921–43932. [[CrossRef](#)]
9. Zhou, J.; Liu, T.; Zhang, H.; Zheng, G.; Qiu, Y.; Deng, M.; Zhang, C.; Yao, G. Anti-inflammatory Grayanane Diterpenoids from the Leaves of *Rhododendron molle*. *J. Nat. Prod.* **2018**, *81*, 151–161. [[CrossRef](#)] [[PubMed](#)]
10. Niu, C.-S.; Li, Y.; Liu, Y.-B.; Ma, S.-G.; Liu, F.; Cui, L.; Yu, H.-B.; Wang, X.-J.; Qu, J.; Yu, S.-S. Grayanane diterpenoids with diverse bioactivities from the roots of *Pieris formosa*. *Tetrahedron* **2018**, *74*, 375–382. [[CrossRef](#)]
11. Sun, N.; Zhu, Y.; Zhou, H.; Zhou, J.; Zhang, H.; Zhang, M.; Zeng, H.; Yao, G. Grayanane Diterpenoid Glucosides from the Leaves of *Rhododendron micranthum* and Their Bioactivities Evaluation. *J. Nat. Prod.* **2018**, *81*, 2673–2681. [[CrossRef](#)] [[PubMed](#)]
12. Kong, L.; Yu, H.; Deng, M.; Wu, F.; Chen, S.C.; Luo, T. Enantioselective Total Syntheses of Grayanane Diterpenoids and (+)-Kalmanol: Evolution of the Bridgehead Carbocation-Based Cyclization and Late-Stage Functional Group Manipulation Strategies. *J. Org. Chem.* **2023**, *88*, 6017–6038. [[CrossRef](#)] [[PubMed](#)]
13. Yu, K.; Yang, Z.N.; Liu, C.H.; Wu, S.Q.; Hong, X.; Zhao, X.L.; Ding, H. Total Syntheses of Rhodomolleins XX and XXII: A Reductive Epoxide-Opening/Beckwith-Dowd Approach. *Angew. Chem. Int. Ed. Engl.* **2019**, *58*, 8556–8560. [[CrossRef](#)] [[PubMed](#)]
14. Li, C.H.; Zhang, J.Y.; Zhang, X.Y.; Li, S.H.; Gao, J.M. An overview of grayanane diterpenoids and their biological activities from the Ericaceae family in the last seven years. *Eur. J. Med. Chem.* **2019**, *166*, 400–416. [[CrossRef](#)] [[PubMed](#)]
15. Cai, Y.Q.; Hu, J.H.; Qin, J.; Sun, T.; Li, X.L. *Rhododendron molle* (Ericaceae): Phytochemistry, pharmacology, and toxicology. *Chin. J. Nat. Med.* **2018**, *16*, 401–410. [[CrossRef](#)] [[PubMed](#)]
16. Zheng, G.; Huang, L.; Feng, Y.; Zhang, H.; Ma, X.; Gao, B.; Sun, Y.; Abudurexiti, A.; Yao, G. Structurally diverse analgesic diterpenoids from the flowers of *Rhododendron molle*. *Fitoterapia* **2024**, *172*, 105770. [[CrossRef](#)] [[PubMed](#)]
17. Sun, N.; Qiu, Y.; Zhu, Y.; Liu, J.; Zhang, H.; Zhang, Q.; Zhang, M.; Zheng, G.; Zhang, C.; Yao, G. Rhodomicrosides A-I, analgesic diterpene glucosides with diverse carbon skeletons from *Rhododendron micranthum*. *Phytochemistry* **2019**, *158*, 1–12. [[CrossRef](#)] [[PubMed](#)]
18. Niu, C.; Liu, S.; Li, Y.; Liu, Y.; Ma, S.; Liu, F.; Li, L.; Qu, J.; Yu, S. Diterpenoids with diverse carbon skeletons from the roots of *Pieris formosa* and their analgesic and antifeedant activities. *Bioorg. Chem.* **2020**, *95*, 103502. [[CrossRef](#)] [[PubMed](#)]
19. Feng, Y.; Zha, S.; Zhang, H.; Gao, B.; Zheng, G.; Jin, P.; Chen, Y.; Yao, G. Rhodauricanol A, an analgesic diterpenoid with an unprecedented 5/6/5/7 tetracyclic system featuring a unique 16-oxa-tetracyclo [11.2.1.0^{1,5}.0^{7,13}]hexadecane core from *Rhododendron dauricum*. *Chin. Chem. Lett.* **2023**, *34*, 107742. [[CrossRef](#)]
20. Jin, P.; Zheng, G.; Yuan, X.; Ma, X.; Feng, Y.; Yao, G. Structurally diverse diterpenoids with eight carbon skeletons from *Rhododendron micranthum* and their antinociceptive effects. *Bioorg. Chem.* **2021**, *111*, 104870. [[CrossRef](#)] [[PubMed](#)]
21. Zheng, G.; Jin, P.; Huang, L.; Zhang, Q.; Meng, L.; Yao, G. Structurally diverse diterpenoids from *Pieris japonica* as potent analgesics. *Bioorg. Chem.* **2020**, *99*, 103794. [[CrossRef](#)] [[PubMed](#)]
22. Chai, B.; Li, Y.; Yu, S.S. Three new antinociceptive diterpenoids from the roots of *Rhododendron micranthum*. *J. Asian Nat. Prod. Res.* **2020**, *22*, 895–904. [[CrossRef](#)] [[PubMed](#)]
23. Li, Y.; Zhu, Y.; Zhang, Z.; Li, L.; Liu, Y.; Qu, J.; Ma, S.; Yu, S. Antinociceptive grayanane-derived diterpenoids from flowers of *Rhododendron molle*. *Acta Pharm. Sin. B* **2020**, *10*, 1073–1082. [[CrossRef](#)] [[PubMed](#)]
24. Sun, N.; Feng, Y.; Zhang, Q.; Liu, J.; Zhou, H.; Zhang, H.; Zheng, G.; Zhou, J.; Yao, G. Analgesic diterpenoids with diverse carbon skeletons from the leaves of *Rhododendron auriculatum*. *Phytochemistry* **2019**, *168*, 112113. [[CrossRef](#)] [[PubMed](#)]
25. Zhu, Y.X.; Zhang, Z.X.; Yan, H.M.; Lu, D.; Zhang, H.P.; Li, L.; Liu, Y.B.; Li, Y. Antinociceptive Diterpenoids from the Leaves and Twigs of *Rhododendron decorum*. *J. Nat. Prod.* **2018**, *81*, 1183–1192. [[CrossRef](#)] [[PubMed](#)]
26. Zhou, J.; Liu, J.; Dang, T.; Zhou, H.; Zhang, H.; Yao, G. Mollebenzylanols A and B, Highly Modified and Functionalized Diterpenoids with a 9-Benzyl-8,10-dioxatricyclo[5.2.1.0^{1,5}]decane Core from *Rhododendron molle*. *Org. Lett.* **2018**, *20*, 2063–2066. [[CrossRef](#)]
27. Huang, L.; Zheng, G.; Feng, Y.; Jin, P.; Gao, B.; Zhang, H.; Ma, X.; Zhou, J.; Yao, G. Highly Oxygenated Dimeric Grayanane Diterpenoids as Analgesics: TRPV1 and TRPA1 Dual Antagonists from *Rhododendron molle*. *Chin. J. Chem.* **2022**, *40*, 2285–2295. [[CrossRef](#)]
28. Sun, N.; Zheng, G.; He, M.; Feng, Y.; Liu, J.; Wang, M.; Zhang, H.; Zhou, J.; Yao, G. Grayanane Diterpenoids from the Leaves of *Rhododendron auriculatum* and Their Analgesic Activities. *J. Nat. Prod.* **2019**, *82*, 1849–1860. [[CrossRef](#)] [[PubMed](#)]
29. Zheng, G.; Zhou, J.; Huang, L.; Zhang, H.; Sun, N.; Zhang, H.; Jin, P.; Yue, M.; Meng, L.; Yao, G. Antinociceptive Grayanane Diterpenoids from the Leaves of *Pieris japonica*. *J. Nat. Prod.* **2019**, *82*, 3330–3339. [[CrossRef](#)] [[PubMed](#)]
30. Feng, Y.; Zhang, H.; Gao, B.; Zheng, G.; Zha, S.; Yao, G. Highly oxygenated grayanane diterpenoids with structural diversity from the flowers of *Rhododendron dauricum* and their analgesic activities. *Bioorg. Chem.* **2023**, *132*, 106374. [[CrossRef](#)] [[PubMed](#)]

31. Li, Q.; Guo, Y.; Wei, D.; Gong, L.; Feng, L.; Dong, X.; Cui, T. Grayanane diterpenoids from *Craibiodendron yunnanense* with anti-inflammatory and antinociceptive activities. *Phytochemistry* **2023**, *212*, 113729. [[CrossRef](#)] [[PubMed](#)]
32. Zheng, G.; Huang, L.; Feng, Y.; Zhang, H.; Gao, B.; Ma, X.; Sun, Y.; Abudurexiti, A.; Yao, G. Discovery of highly functionalized grayanane diterpenoids from the flowers of *Rhododendron molle* as potent analgesics. *Bioorg. Chem.* **2024**, *142*, 106928. [[CrossRef](#)] [[PubMed](#)]
33. Wang, M.; Wang, Y.N.; Wang, H.Q.; Yang, W.Q.; Ma, S.G.; Li, Y.; Qu, J.; Liu, Y.B.; Yu, S.S. Minor terpenoids from the leaves of *Craibiodendron yunnanense*. *J. Asian Nat. Prod. Res.* **2023**, *25*, 617–626. [[CrossRef](#)] [[PubMed](#)]
34. Niu, C.S.; Li, Y.; Liu, Y.B.; Ma, S.G.; Wang, X.J.; Liu, F.; Liu, S.; Qu, J.; Yu, S.S. Diverse epoxy grayanane diterpenoids with analgesic activity from the roots of *Pieris formosa*. *Fitoterapia* **2019**, *133*, 29–34. [[CrossRef](#)] [[PubMed](#)]
35. Zhang, R.; Tang, C.; Ke, C.-Q.; Yao, S.; Lin, G.; Ye, Y. Bihodomolleins D and E, two new dimeric grayanane diterpenes with a 3-O-2' linkage from the fruits of *Rhododendron pumilum*. *Chin. Chem. Lett.* **2018**, *29*, 123–126. [[CrossRef](#)]
36. Feng, Y.; Zha, S.; Gao, B.; Zhang, H.; Jin, P.; Zheng, G.; Ma, Y.; Yao, G. Discovery of Kalmene Diterpenoids as Potent Analgesics from the Flowers of *Rhododendron dauricum*. *Chin. J. Chem.* **2022**, *40*, 1019–1027. [[CrossRef](#)]
37. Hanson, J.R. From 'mad honey' to hypotensive agents, the grayanoid diterpenes. *Sci. Prog.* **2016**, *99*, 327–334. [[CrossRef](#)] [[PubMed](#)]
38. Yang, J.; Yang, Q.; Zhao, J.; Sun, S.; Liu, M.; Wang, Y.; Feng, Y.; Zhang, J. Evaluation of Rhodojaponin III from *Rhododendron molle* G. Don. on oral antinociceptive activity, mechanism of action, and subacute toxicity in rodents. *J. Ethnopharmacol.* **2022**, *294*, 115347. [[CrossRef](#)] [[PubMed](#)]
39. Lukowski, A.L.; Narayan, A.R.H. Natural Voltage-Gated Sodium Channel Ligands: Biosynthesis and Biology. *Chembiochem* **2019**, *20*, 1231–1241. [[CrossRef](#)]
40. Chen, R.; Wang, M.; Keasling, J.D.; Hu, T.; Yin, X. Expanding the structural diversity of terpenes by synthetic biology approaches. *Trends Biotechnol.* **2024**. [[CrossRef](#)] [[PubMed](#)]
41. Singh, S.; Grewal, A.S.; Grover, R.; Sharma, N.; Chopra, B.; Dhingra, A.K.; Arora, S.; Redhu, S.; Lather, V. Recent updates on development of protein-tyrosine phosphatase 1B inhibitors for treatment of diabetes, obesity and related disorders. *Bioorg. Chem.* **2022**, *121*, 105626. [[CrossRef](#)] [[PubMed](#)]
42. Zhang, P.; Wu, G.; Heard, S.C.; Niu, C.; Bell, S.A.; Li, F.; Ye, Y.; Zhang, Y.; Winter, J.M. Identification and Characterization of a Cryptic Bifunctional Type I Diterpene Synthase Involved in Talaronoid Biosynthesis from a Marine-Derived Fungus. *Org. Lett.* **2022**, *24*, 7037–7041. [[CrossRef](#)]
43. Škubník, J.; Pavlíčková, V.; Ruml, T.; Rimpelová, S. Current perspectives on taxanes: Focus on their bioactivity, delivery and combination therapy. *Plants* **2021**, *10*, 569. [[CrossRef](#)] [[PubMed](#)]
44. Chen, Y.; Zhu, Z.; Chen, J.; Zheng, Y.; Limsila, B.; Lu, M.; Gao, T.; Yang, Q.; Fu, C.; Liao, W. Terpenoids from *Curcumae Rhizoma*: Their anticancer effects and clinical uses on combination and versus drug therapies. *Biomed. Pharmacother.* **2021**, *138*, 1113504. [[CrossRef](#)] [[PubMed](#)]
45. Liu, F.; Wang, Y.-N.; Li, Y.; Ma, S.-G.; Qu, J.; Liu, Y.-B.; Niu, C.-S.; Tang, Z.-H.; Zhang, T.-T.; Li, Y.-H. Rhodoterpenoids A–C, Three New Rearranged Triterpenoids from *Rhododendron latoucheae* by HPLC–MS–SPE–NMR. *Sci. Rep.* **2017**, *7*, 7944. [[CrossRef](#)] [[PubMed](#)]
46. Liu, F.; Wang, Y.-N.; Li, Y.; Ma, S.-G.; Qu, J.; Liu, Y.-B.; Niu, C.-S.; Tang, Z.-H.; Li, Y.-H.; Li, L. Triterpenoids from the twigs and leaves of *Rhododendron latoucheae* by HPLC–MS–SPE–NMR. *Tetrahedron* **2019**, *75*, 296–307. [[CrossRef](#)]

Disclaimer/Publisher's Note: The statements, opinions and data contained in all publications are solely those of the individual author(s) and contributor(s) and not of MDPI and/or the editor(s). MDPI and/or the editor(s) disclaim responsibility for any injury to people or property resulting from any ideas, methods, instructions or products referred to in the content.